Climate Change and Unemployment Dynamics: Evidence from U.S. Counties*

W. Similan Rujiwattanapong† Masahiro Yoshida‡

February 5, 2026

Abstract

Seasonal adjustment removes 80% of within-year variation in unemployment. Linking local weather to unadjusted monthly unemployment rates at the U.S. county level from 1990 to 2019, we find that unemployment would have been 11% lower on average absent extreme temperature days, whereas their effect on seasonally-adjusted series is largely obscured. The effect primarily operates through fewer job openings and hiring, alongside higher separations—especially layoffs—resulting in greater unemployment insurance recipiency and a slacker labor market. We then quantify the nationwide implications of long-run climate change: while milder winters have reduced unemployment, these gains are eroded by accelerating summer unemployment.

Keywords: Climate change, Unemployment, Seasonal adjustment

JEL Codes: J64, J63, Q54, E24, C23

*We thank Benjamín Villena-Roldán and Empirical Micro and Macro seminar participants at Waseda for insightful comments. This paper is a substantially revised version of an earlier manuscript, circulated as Rujiwattanapong and Yoshida (2025) (WINPEC Working Paper No. E2512, May 2025).

†Faculty of Political Science and Economics, Waseda University and Centre for Macroeconomics. Email: sruji@waseda.jp. Webpage: sites.google.com/site/wsrujiwattanapong.

‡Corresponding author. Faculty of Political Science and Economics, Waseda University, Tokyo. Email: m.yoshida@waseda.jp. Webpage: www.m-yoshida.com.

"Unemployment is like a headache or a high temperature—unpleasant and exhausting but not carrying in itself any explanation of its cause."

—William Henry Beveridge, *Causes and Cures of Unemployment* (1931)

1 Introduction

Since the Great Depression in the 1930s, unemployment has been a critical input to policy debates (e.g., fiscal and monetary policy; minimum wage), consistently monitored as a "temperature" of the economy (Beveridge (1931)). This centrality reflects its substantial real-world consequences—disrupting consumption smoothing (Gruber (1997)), impairing mental health (Eliason and Storrie (2009)), and even elevating risks of crimes (Raphael and Winter-Ebmer (2001)) and suicides (Milner et al. (2013)). Our inquiry starts from a routinely overlooked premise that joblessness is highly seasonal: the peak-to-trough of the recent seasonal component of unemployment matches half of the seasonally adjusted (SA) spike in the Great Recession (Figure 1a1). In non-recession years, seasonal unemployment accounts for nearly 80% of the within-year variation in the non-seasonally adjusted (NSA) unemployment rate (Figure 1a2).

Despite strong policy interest in the real-time release and short-term forecasting of unemployment rates, economists—who place considerable emphasis on underlying trends and cycles—conventionally smooth out the series through seasonal adjustment (Stock and Watson (1999); Hodrick and Prescott (1997)). In line with this tradition, little attention is paid to the regularity and mechanisms of high-frequency, NSA unemployment dynamics. As a first step toward uncovering the "black box", this paper directly relates regional NSA unemployment rates to arguably the most prominent seasonal factor—temperature—which fluctuates markedly across time and space. We then assess the long-run implications of climate change for nationwide unemployment dynamics, given the accelerated warming since around 2000.

We begin by comparing seasonal changes in the unemployment rate in summer and winter with their corresponding temperature exposures. Figure 1b plots nationwide experience of hot days in second-third quarters (Q2–Q3) and cold days in previous fourth-first quarters (pre Q4–Q1), respectively[1], alongside the half-year change of NSA unemployment rates in 1950–2019. Despite the limited sample of 70 years, we find statistically significantly positive slopes ($t = 2$).[2] Guided by the historical associations, we hypothesize that the arrival of hot summers and cold winters elevate unemployment rates. First, extreme temperature days would significantly hurt labor efficiency (see a survey on Lai et al. (2023)), for example, by increasing fatigue, absenteeism, operational errors, and workplace injury risk, and thereby, reducing labor demand.

[1] Exposure to hot and cold days in each county is averaged using contemporaneous county labor force weights.
[2] Including or excluding recession years does not significantly change the estimate.

Figure 1: Nationwide Trend: Unemployment Dynamics in the U.S. (1950–2019)

(a) Seasonal vs. Seasonally-adjusted Unemployment Rate

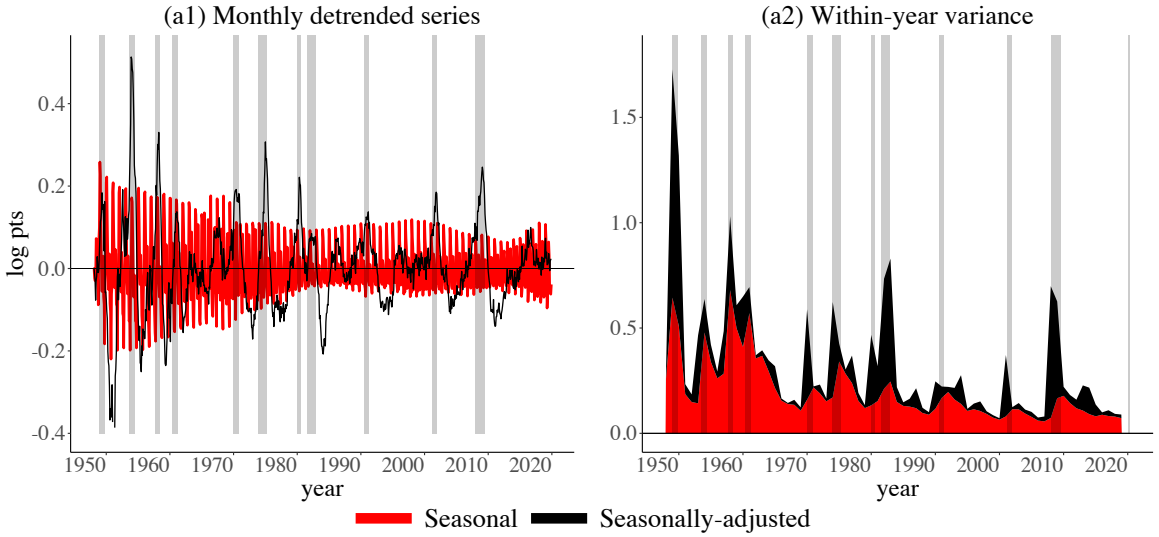

(b) Half-year Temperature Shocks and Unemployment Swings

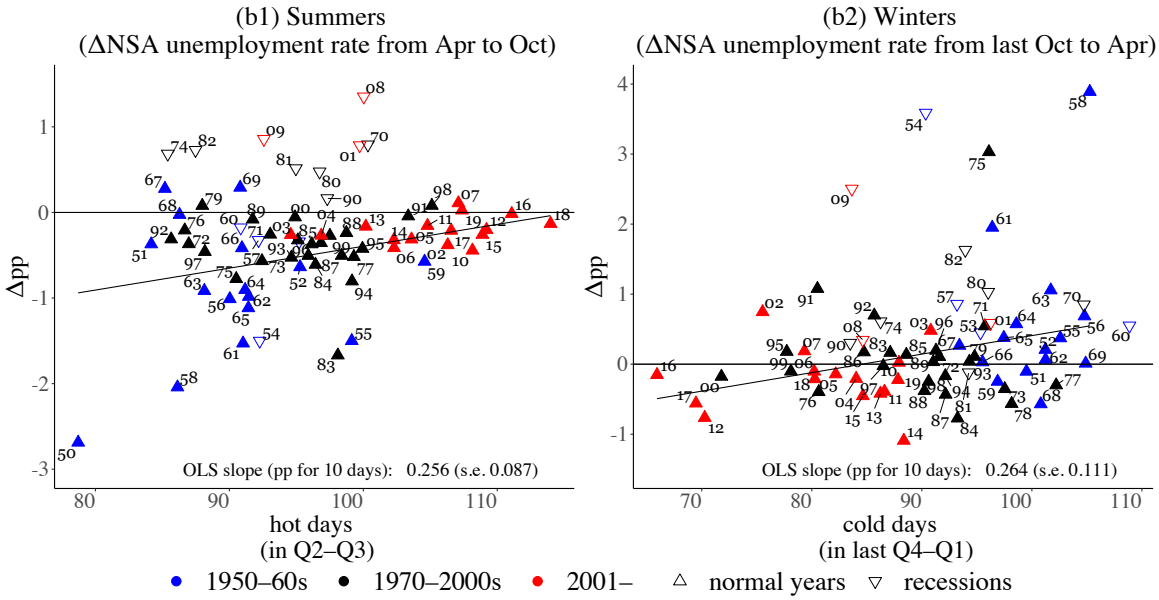

Notes: Panel (a) Nationwide seasonal unemployment rate is a gap between non-seasonally adjusted (NSA) and seasonally adjusted (SA) monthly headline figures of unemployment rate from the Bureau of Labor Statistics (BLS).
Panel (a1): Seasonal and SA monthly unemployment rates are detrended by Hodrick-Prescott filter with a smoothing parameter $\lambda = 14,400$. Panel (a2): The variance of monthly seasonal and SA unemployment rates within each year (percentage points, pp).
Panel (b): NSA monthly unemployment rates are differenced between April and October. County-level exposure to hot and cold days (a daily working-hour temperature above 75°F and below 50°F) over the two consecutive quarters, are aggregated nationwide, weighted by county labor force. The fitted lines are trends without recession years, identified by NBER-dated recession periods.

Second, temperature shocks also hamper production activities (Cachon et al. (2012); Chen and Yang (2019)) through, for example, supply-chain delays, electricity shortages, and machine failures. These channels operate through both fewer hiring and more separations.

To formally test this hypothesis, we build a new spatial panel data connecting plausibly-random monthly-level exposure to binned temperature and NSA unemployment rates across U.S. counties during 1990–2019, allowing for the standard identification under the two-way fixed effects (see Dell et al. (2014)). Through year-month fixed effects, temperature impacts are isolated from the nationwide business cycle and calendar effects (e.g., annual contracts and school graduation). We find that 10 more extreme temperature days per month (hot days over 75°F or cold days below 50°F) increase the unemployment rate by 0.2–0.3 percentage points. The results are robust to reasonable combinations of fixed effects and to the inclusion of additional weather variables (e.g., rainfall, snowfall, and humidity). Notably, relationships with SA unemployment rates are substantially muted, suggesting that climate-induced unemployment is predominantly concentrated in the often-overlooked seasonal component.

Equipped with the model, we then turn to assess the role of extreme temperatures and warming since around 1980. The back-of-the-envelope calculation corroborates that temperature is a non-negligible driver of unemployment: absent extreme temperature days, the average NSA unemployment rate over 2000–2019 would have been 11.4% lower, whereas the impact on the seasonally adjusted series is 0.42%. The impacts are largely driven by hot summer days, which are more prevalent in Southern states. Alongside global warming, we document that the volatility of seasonal unemployment has steadily declined (Figure 1a). By comparing the pre-warming decades (1950–1979) with the new century (2000–2019), we estimate that warming temperatures account for 5.6% of the reduction in the variance of NSA unemployment rates. This is due to milder winters that lower winter unemployment peaks, combined with harsher summers that elevate the summer unemployment floor at an accelerating pace.

To unpack the underlying mechanisms and inform the policy responses, we provide three complementary analyses. First, tracking the quarterly job flows at county-by-industry level during 2000–2019, we find that exposure to hot and cold days reduces job creation and suppresses the labor market dynamism. Hot days slightly increase job destruction, while cold days mitigate it. Second, investigating state-level quarterly worker-flows, we also find that hot days slacken the labor market primarily by reducing hiring through fewer job openings, and secondarily by raising separations—especially layoffs. Third, we find that statewide unemployment insurance receipt—largely triggered by involuntary job loss—is also shaped by extreme temperature, reinforcing the contraction in labor demand documented in the first two results. Looking ahead, projected temperature warming (IPCC (2023)) is expected to intensify fiscal burdens through greater summer unemployment.

Related Literature. Connecting unemployment with climate variables, this paper contributes to the intersections of macroeconomics, labor economics and climate science. First, the paper proposes climate change as a novel determinant of unemployment dynamics. Economists conventionally analyze unemployment as a consequence of spatial exposure to trade shocks (Autor et al. (2013); Kim and Vogel (2021)), tariffs (Furceri et al. (2018)), industrial robots (Acemoglu and Restrepo (2020)), mass layoffs (Gathmann et al. (2020); Black et al. (2005)), and UI regime (Chodorow-Reich et al. (2019); Rujiwattanapong (2025)). Our paper is the first to empirically associate regional unemployment with climatic temperature, varying across both time and space.[3] Importantly, our climate impacts are not captured in seasonally-adjusted or annualized data, the basis of nearly all prior studies. We provide a deeper understanding of real-time unemployment rates—headline indicators of macroeconomic climates—by revealing their hidden sensitivity to contemporaneous temperature exposure.

Second, this paper adds to the small body of research uncovering seasonality of the macroeconomy (Barsky and Miron (1989); Beaulieu and Miron (1992)) and employment (Coglianese and Price (2025); Price and Wasserman (2024); Geremew and Gourio (2018)). A unified theme of the literature is that routinely smoothed away seasonal statistics has a substantial real-world implication. None of these analyzed unemployment. Despite the conventional view that unemployment seasonality is a stable, recurring cycle that can be smoothed out, we find that it is time-varying and generally shrinking, partly driven by climate change. In parallel with the stability of the SA unemployment rate during Great Moderation after 1984 (see Galí and Gambetti (2009)), our finding suggests that the *de facto* moderation in the NSA unemployment rate was even greater.

Third, the proposed mechanism of climate-induced unemployment builds on empirical works on productivity losses at the factory level (Chen and Yang (2019); Zhang et al. (2018); Cachon et al. (2012); Somanathan et al. (2021)) and the worker level (efficiency damage for Borg et al. (2021); Hancock et al. (2007)); shrinking hours of work for Ireland et al. (2025); Graff Zivin and Neidell (2014)). We approach unemployment dynamics through employment *flows*, primarily characterized by suppressed hiring at the state level. Our flow-based evidence complements the burgeoning works on adaptations to climate change: employee reallocation by multi-county firms (Acharya et al. (2023)), exits of small factories (Ponticelli et al. (2023)), capital deepening and technological change (Xiao (2021); Ma (2025)). While consistent with this micro-level evidence on firms, factories, and workers, our paper highlights regional labor demand dynamics with nationwide implications for unemployment.[4]

[3] A notable recent exception, Kim et al. (2025) analyze the effects of temperature shocks on nationwide macroeconomic statistics, including output, prices and unemployment rates. They employ a time-series method to leverage intertemporal variation of the macro climate shocks, while we also exploit their intranational spatial variation at the county level.

[4] The paper also belongs to the growing literature on climate and the macroeconomic outcomes (see Bilal

The remainder of the paper is structured as follows. Section 2 describes the key data sources and our econometric framework. Section 3 presents the baseline results and robustness checks. Then, we evaluate the role of climate change in the magnitude and dynamics of unemployment. Section 4 explores the mechanism through employment flows. Section 5 discusses an implication for unemployment insurance recipiency. Section 6 concludes. The Appendix reports additional figures and tables (labeled with "A").

2 Data and Model

2.1 Weather and Climate

We construct daily temperature at the county level, using weather station data from the Global Historical Climatology Network Daily (GHCN-Daily), managed by the National Climatic Data Center (NCDC) of the National Oceanic and Atmospheric Administration (NOAA). The GHCN-Daily database provides daily climate statistics, such as maximum and minimum daily temperature, precipitation, and snowfall, from approximately 15,000 weather stations across the U.S., offering a comprehensive climatic dataset with the highest frequency, resolution, and quality since the 19th century. We use the data from stations with complete annual records during 1950–2019.

County-level temperature. To aggregate station-level data to the county level, we employ an inverse-distance weighting method (e.g., Barreca et al. (2016)). Specifically, we aggregate the daily records of the three nearest weather stations to the county's population centroid, weighted by the inverse square of the distance from the centroid. Then, we construct an average daytime temperature for each day d as a weighted average of the maximum and minimum temperature, i.e., $T_d = \omega T_d^{\max} + (1-\omega) T_d^{\min}$. Instead of using $\omega = 0.5$ as is common in the climate literature, we assign $\omega = 0.75$ in light of our focus on regular working hours, 8 am to 6 pm.[5] We find a substantial geographical variation of exposure to climate change across counties even within states (Figure A-2).

and Stock (2025) for a survey) such as growth (Dell et al., 2012; Colacito et al., 2019), income (Deryugina and Hsiang (2014)), labor share (Qiu and Yoshida (2024)) and labor force participation (Yoshida (2025)).

[5]This calculation assumes a linear fluctuation of temperature between its minimum at 6 am and its maximum at 1:30 pm.

2.2 Unemployment

Unemployment rate. We construct unemployment rates from both NSA and SA civilian unemployment and employment (ages 16 and above) at the county-year-month level in the U.S. mainland during 1990–2019 from the Local Area Unemployment Statistics (LAUS). The dataset is produced by the Bureau of Labor Statistics (BLS) from the Current Population Survey, the Current Employment Statistics (CES) survey, and state unemployment insurance (UI) systems.

Employment flows. We draw on local employment flows—job flows (creation and destruction) and worker flows (separations and hires)—at the county-industry-year-quarter level for 19 NAICS private industries over 1993–2019, using data from the Quarterly Workforce Indicators (QWI). This dataset is constructed from the Longitudinal Employer-Houshold Dynamics (LEHD) by the Census Bureau—employer-employee linked massive longitudinal microdata covering over 95% of U.S. private sector jobs.

Worker flows. We obtain worker flows of separations (divided into layoffs and quits) and hires as well as job openings at the state-year-month level from December 2000 to December 2019 for 48 states plus D.C. from the Job Openings and Labor Turnover Survey (JOLTS). This dataset is constructed from a monthly survey of approximately 21,000 U.S. business establishments in all nonagricultural industries, collected by the BLS.

2.3 Seasonal Regularity in Unemployment

We codify the observed dynamic and spatial patterns of seasonal unemployment into three stylized facts (Facts 1–3), which we then empirically relate to extreme temperature.

Fact 1: Unemployment rate spikes in the summer (Q3) and winter (Q1) quarters. Figure 2a1 illustrates the nationwide changes in the seasonal unemployment rate before and after the recessionary peak in 1984, computed as the difference between the BLS-based NSA and SA unemployment rates. Traditionally, the nationwide unemployment rate spikes in January from the previous December, presumably reflecting the end of annual contracts in fiscal years and holiday shopping seasons. A notable pattern is the spike in unemployment from May to June, the onset of summer, coinciding with graduation and summer breaks when high school or college students search for jobs. Especially since 1984, the June spike has been followed by a more gradual decline, with unemployment remaining elevated through Q3. Taken together, the unemployment rate surges in winter (Q1) and summer (Q3) quarters, when temperatures hit their lowest and highest.

Fact 2: Hotter (colder) states experience a larger increase in summer (winter) unemployment. Taking a spatial perspective, Figure 2c examines the climate-unemployment dynamics across states, split between summer and winter over 1990–2019. In the summer, hotter states (e.g., Florida, Arizona, and Texas) experienced a larger increase (or a smaller decrease) in unemployment rates relative to colder states (e.g., Minnesota, Michigan, and Wisconsin). In contrast, in the winter, colder states experienced a larger increase in unemployment rates relative to hotter states.[6] Both relationships are consistent with our proposition that seasonal climate shocks raise regional unemployment rates.

Fact 3: Unemployment seasonality has been shrinking. The magnitude of the seasonal component of the monthly unemployment rate consistently shrinks over time (Figure 1a). Within a year, Figure 2a shows that this declining seasonal volatility largely reflects a steady fall in Q1 unemployment (Jan–Mar) and a gradual rise in Q3 unemployment (Jul–Sep). This pattern of unemployment dynamics aligns well with climate change, marked by fewer cold days in Q1 and more hot days in Q3 (Figure 2b). Intriguingly, we find that the shrinkage of unemployment seasonality is observed not only in the U.S., but also in Canada, Germany, and, more broadly, across OECD countries (Figure A-4), spanning diverse institutional settings and climatic conditions—suggestive of a role for global warming. Overall, Figure 2 summarizes dynamic and spatial variation as sources of identification, which we formally implement below.[7]

2.4 Model

To test climate-induced unemployment, we build and estimate the baseline model that relates county-level monthly NSA unemployment rates to climate exposure, with two-way fixed effects. Specifically, for county l in year $t \in \{1990, \cdots, 2019\}$ and month $m \in \{1, \cdots, 12\}$, we run:

$$\text{UnempRate}_{l,t,m} = \sum_{b \in \{1,\cdots,10,13,\cdots,16\}} \beta^b \text{days}^b_{l,t,m} + \mathbf{\Lambda C}_{l,t,m} + \delta_l + \delta_{t,m} + \varepsilon_{l,t,m}, \tag{1}$$

where $\text{UnempRate}_{l,t,m}$ is county l's unemployment rate in year t and month m. $\text{days}^b_{l,t,m}$ is a number of days falling into 5°F temperature bin indexed by $b \in \{1, \cdots, 10, 13, \cdots, 16\}$ in month m, where the missing 11th and 12th bins (65–75°F) are set as benchmarks.[8] We also control for

[6] A positive link is also observed across commuting zones (Figure A-5).

[7] We find that the seasonality of employment-to-population ratio mirrors Fact1-3 (Figure A-6).

[8] We use 65–75°F as the benchmark temperature range for three reasons. First, OSHA recommends temperature control in the range of 68-76°F for indoor workplaces. Second, Chen and Yang (2019) find that establishment-level industrial output declines when the daily temperature exceeds 24°C (75.2°F). Finally, a clear jump in the estimated temperature effect at 75°F ensures that temperatures above this threshold are sufficiently "hot" relative to the benchmark.

Figure 2: Climate Change and Seasonal Unemployment in the U.S.

(a) Seasonal Unemployment

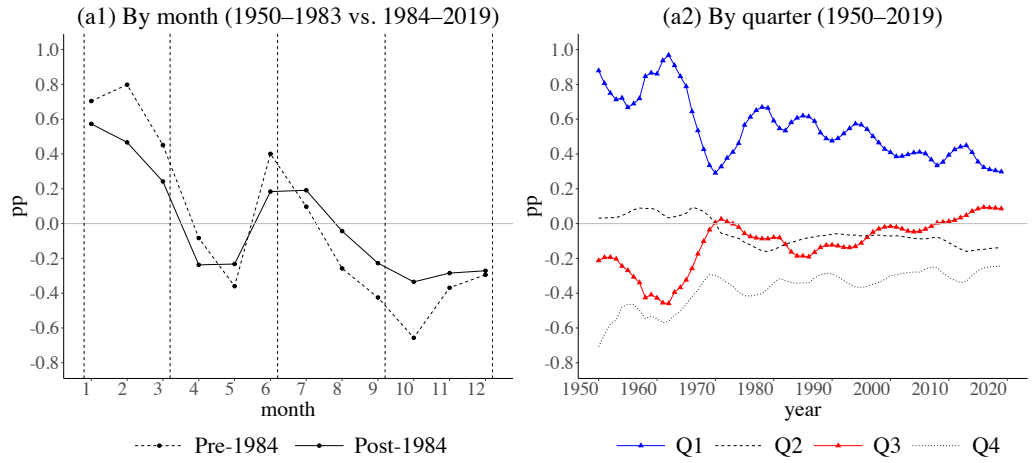

(b) Climate Change

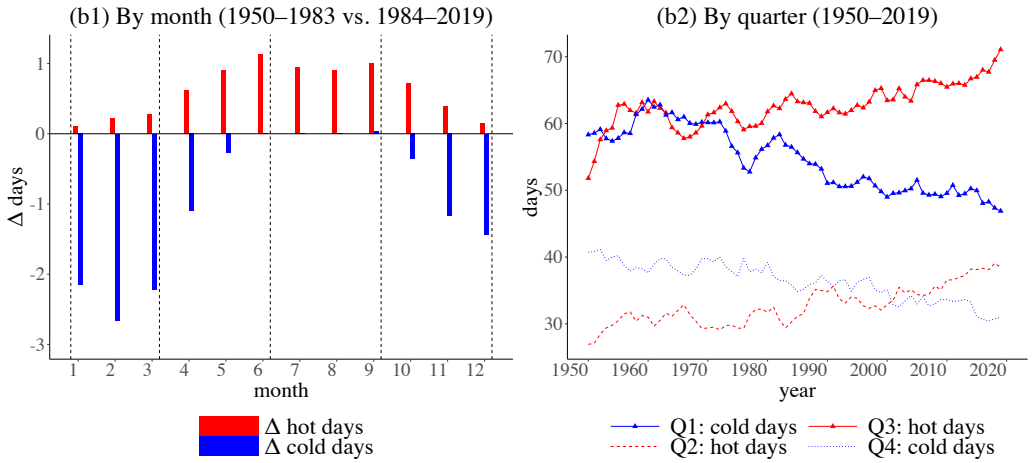

(c) Temperature Shocks and Seasonal Unemployment Rate Swings
(ΔNSA unemployment rate within states averaged over 1990–2019)

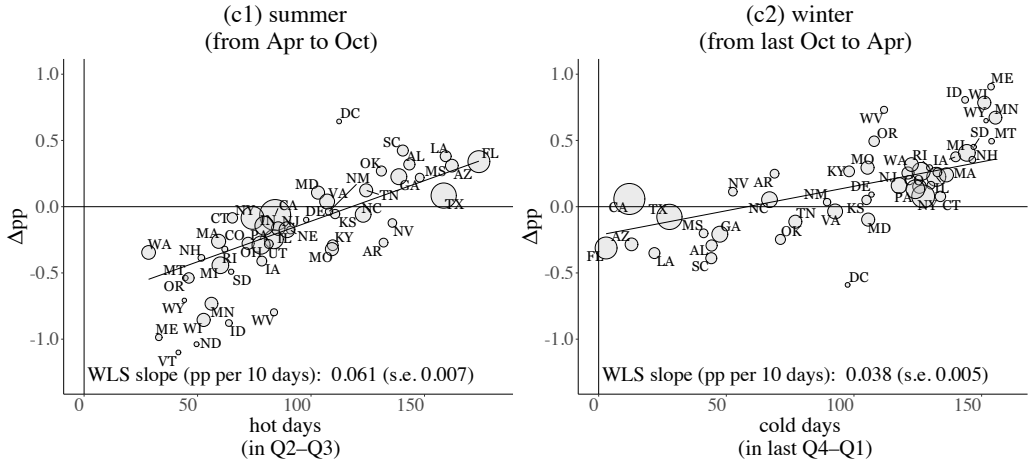

Notes: Panel (a): Within a month or a quarter, seasonal unemployment rate is a difference of NSA and SA nationwide series provided by the BLS. (a1): Change in average seasonal monthly rates, 1950–1983 vs. 1984–2019. (a2): 5-year moving average of quarterly seasonal rates. Panel (b): Within a month or a quarter, county-level exposure to hot and cold days (above 75°F and below 50°F for a daily working-hour temperature), are aggregated nationwide, weighted by county labor force. (b1) Change in average monthly exposure to hot and cold days, 1950–1983 vs. 1984–2019. (b2) Hot and cold days by quarter are 5-year moving averages. Panel (c): County-level exposure to analogously defined hot and cold days is aggregated to states plus D.C. averaged during 1990–2019, weighted by county labor force. The fitted lines are weighted by period-average state-level labor force, represented by the bubble size.

rainy days in additional climate covariates $\mathbf{C}_{l,t,m}$ and county fixed effects δ_l. The year-month fixed effects $\delta_{t,m}$ capture any time-varying nationwide shocks (e.g., business cycles, technological change, and free trade) as well as monthly calendar effects (e.g., fiscal-year contracts). The regression is weighted by the logarithm of labor force of each county and standard errors are clustered at the commuting-zone (i.e., superset of neighboring counties) level.[9] Presuming that temperature shocks are unconditionally random, β^b captures the effect of ten days in each bin, relative to ten benchmark-temperature days of 65–75°F. While we rely on the simplest one-month treatment window to estimate contemporaneous temperature effects, we also consider an augmented model that incorporates lagged effects from prior months, thereby quantifying cumulative impacts over time (Section 3.2).

3 Results

Semi-parametric bin models. Figure 3a1 illustrates our baseline results. The red line of the top figure plots the U-shaped response of the NSA unemployment rate to each temperature bin of 10 days with 95% confidence intervals. On average, a 10-day increase of hot days (≥75°F) or cold days (<50°F) per month increases the unemployment rate by 0.2–0.3 percentage points (pp).[10] Importantly, we find largely muted effects on the commonly-used SA unemployment rate, suggesting that our estimates predominantly capture within-year seasonal impacts (Figure 3a2). Additionally, consistent with the U-shaped estimates, we also find that the effects are amplified in historically hot (e.g., Southeast) and cold (e.g., Northeast) regions that are more exposed to extreme temperature (Table A-6).

Figure 3b analyzes the responses of unemployment, employment, and out of the labor force separately, expressed as ratios to the population.[11] The decline in employment is roughly twice as large as the increase in unemployment, implying that about half of employment separations translate into exits from the labor force—likely reflecting quits by employed workers (including temporary seasonal workers) as well as labor force withdrawal among discouraged unemployed workers.

[9] We find that the estimates are robust against alternative clustering options (Figure A-9).

[10] We find that precipitation or snowfall significantly raises unemployment, likely reflecting disruptions to business operations (Table A-3).

[11] Because the county-level monthly data on the out-of-labor-force population are unavailable, we impute the series as the difference between the annualized population (ages 15+) from the SEER data and the monthly labor force (ages 16+) from the BLS.

Figure 3: Temperature Shocks and Unemployment

(a) Temperature Shocks Predominantly Elevate Unadjusted Unemployment Rates

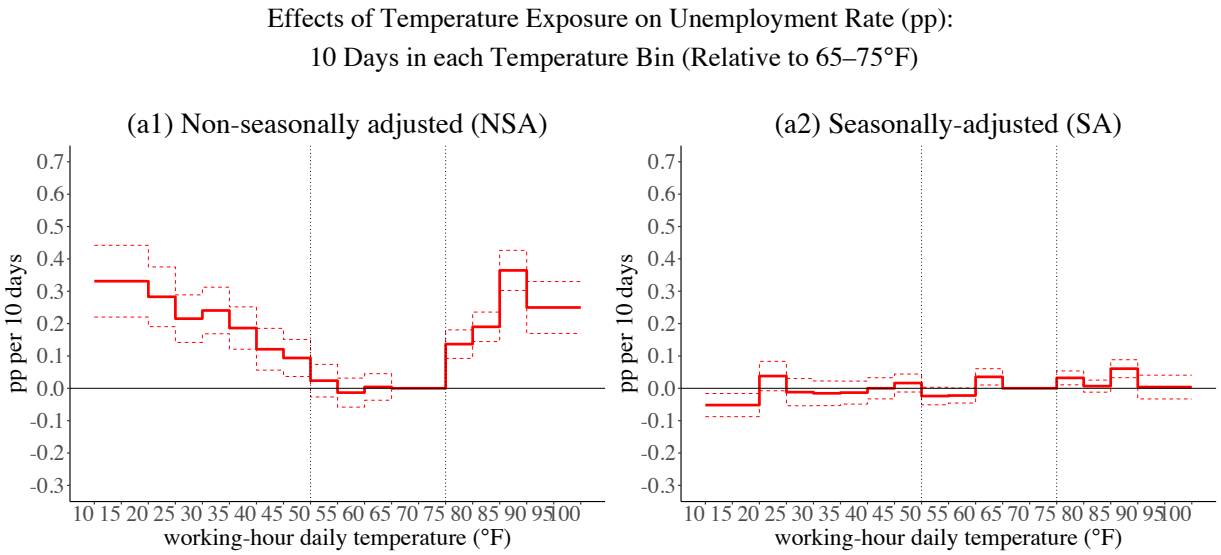

(b) Unemployment vs. Employment and Out-of-Labor-Force as a Ratio-to-Population

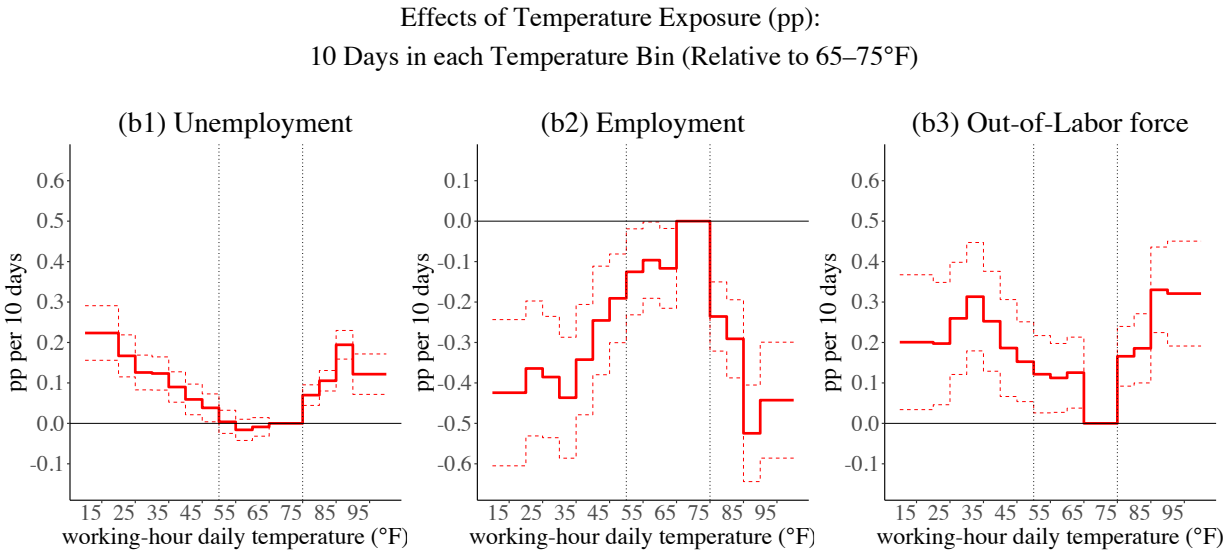

Notes: Unit of analysis: counties × years × months. Eq.(1) is estimated with different outcome variables. Rainy days are controlled for, along with county fixed effects and year-month fixed effects. The regressions are weighted by the log of labor force. Dotted lines are 95% confidence intervals, constructed from standard errors clustered by commuting zone. Bins with 65–75°F are set as the benchmark. An unemployment rate is computed using county-level NSA and SA monthly unemployment and employment series (ages 16+) from the BLS. County population data (ages 15+) comes from the SEER program of the National Cancer Institute. The out-of-labor-force population is imputed as the difference between the population and the labor force.

3.1 Robustness

Fixed effects. The baseline model (Eq.(1)) adopts the standard two-way (county and year-month) fixed effects. The granularity of the data permits an inclusion of county-by-year fixed effects $\delta_{l,t}$ rather than county fixed effects δ_l. The temperature estimates remain largely unchanged, suggesting that they primarily reflect within-year seasonal impacts—consistent with the very modest estimates when the SA unemployment rate is used (Figure 3a2). Controlling for state-by-year fixed effects produces similar temperature estimates, suggesting that time-varying institutional factors (e.g., UI, minimum wage, and unionization) do not critically confound the estimates. We try reasonable alternative combinations of fixed effects, but the estimates remain broadly stable (Figure A-7; Table A-2).

Additional weather variables. The baseline model (Eq.(1)) includes monthly rainy days in additional weather variables, $\mathbf{C}_{l,t,m}$. We consider a reasonable alternative set of weather variables consisting of rainfall, snowfall, and humidity, but the temperature estimates are broadly preserved. Replacing hot days by "uncomfortable days", defined as days with a heat index above 80°F that interact temperature with relative humidity, yields larger and more precise estimates, consistent with the mechanism of declining labor efficiency due to thermal stress (Figure A-8; Table A-3).

Two-tailed models under alternative temperature cutoffs. To ensure tractability in testing the mechanism and to retain sufficient precision for impact quantification, we introduce a simplified two-tailed models:[12]

$$\text{UnempRate}_{l,t,m} = \beta^h \text{hd}_{l,t,m} + \beta^c \text{cd}_{l,t,m} + \mathbf{\Lambda C}_{l,t,m} + \delta_l + \delta_{t,m} + \varepsilon_{l,t,m}, \tag{2}$$

where $\text{hd}_{l,t,m}$ and $\text{cd}_{l,t,m}$ denote hot and cold days, defined as days with average working-hour temperatures above 75°F and below 50°F, respectively, guided by the U-shaped estimates in Figure 3a1.[13] We obtain $\beta^h = 0.240$ (s.e. 0.026) and $\beta^c = 0.248$ (s.e. 0.026), both precisely estimated. Importantly, the coefficients remain statistically significant across alternative reasonable temperature cutoffs (Table A-1).

Two-tailed models with lagged weather variables. As unemployment is potentially affected by climate shocks from previous months, we examine cumulative lag specifications from 0 to M

[12] A two-tailed model has been a standard, tractable complement to binned models in the climate literature, as in Barreca et al. (2016) and Somanathan et al. (2021).

[13] Note that these cutoffs are constructed based on the average temperature during working hours, with the corresponding maxima and minima are higher and lower, respectively.

months ($M \in \{0, \cdots, 5\}$) and find significant lagged estimates, indicating cumulative nature of temperature effects operating within a seasonal time window (Table A-4). This finding cautions against the widely used practice of moving-average smoothing (e.g., over a quarter or half year) for seasonal adjustment of unemployment rates, as lagged effects of past climate shocks remain embedded in the smoothed series (Table A-5).

3.2 Quantitative Assessment

Climate-induced unemployment. Having established the link between temperature and unemployment, we quantitatively assess how exposure to regional extreme temperatures contributes to nationwide non-seasonally-adjusted (NSA) unemployment over the study period, 1990–2019. Because current unemployment may reflect climate shocks from preceding months through frictions in labor demand adjustment, we employ estimates from a two-tailed lagged model with a quarterly time window—corresponding to lags of up to two months—for hot, cold, and rainy days (see Column 3 of Table A-4, introduced above at Section 3.1).[14]

We construct the counterfactual scenario in which all the days fell into normal (non-hot, non-cold) days, and measure the resulting gap between the simulated and empirical unemployment series. Figure 4a illustrates the simulated impacts of extreme temperature days over 1990–2019. Reflecting larger and more persistent lagged effects of hot days (Table A-4), the aggregate impact is primarily driven by the surge in summer unemployment. We also find a pronounced regional heterogeneity: Southern states experience larger impacts from hot days in summer, while Northern states face larger impacts from cold days in winter.[15]

The back-of-the-envelope calculation suggests that temperature is a non-negligible driver of unemployment: absent extreme temperature days, the NSA unemployment rate during non-recessionary periods over 2000–2019 would have been 11.4% lower, while the corresponding reduction in the SA series is only 0.42%.[16] Under a quarterly treatment window, the magnitude remains robust, ranging from 10 to 13%, across protocols (Figure A-11). The contribution of extreme temperatures exhibits substantial seasonal dispersion, ranging from 7.6% in May to 17.8% in September. Because our model does not explicitly incorporate natural disasters (e.g.,

[14]Because simulated temperature impacts expand with wider treatment windows—albeit with less precise estimates at longer lags (Table A-4)—we view this exercise as providing a reasonable lower bound on extreme temperature effects.

[15]Southern states comprise 18 states across the Southeast, South, Southwest and West, accounting for nearly half of the nationwide labor force over 2000–2019.

[16]Because baseline cold-day effects on the SA series cannot be statistically distinguished from zero, we only include hot-day effects (Table A-1).

hurricanes, arctic blasts, wildfires)[17], which are partially captured by precipitation measures,[18] we regard our estimates as a reasonable lower bound on climate-induced unemployment.

Climate change and unemployment dynamics. Given the tangible role of extreme temperatures in regional unemployment, we next address our central question: how the acceleration of climate change since 2000 has reshaped nationwide unemployment. Using the two-tailed lagged model with a quarterly treatment window (Column 3 of Table A-4), we simulate the counterfactual climate impacts across decades—1980s, 1990s, 2000s, 2010s—by keeping the weather exposure fixed at its pre-warming (1950–1979) average to gauge the impacts of climate change.

Figure 4b illustrates the results. We find that a rising frequency of hot days elevates unemployment throughout the year, with the strongest effects in the summer quarter (Q3). By contrast, fewer cold days modestly reduce unemployment. Relative to the 1950s–1970s benchmark, fewer cold days over 2000–2019 reduce winter (Q1) unemployment by 0.022 pp. but more hot days raise summer (Q3) unemployment by 0.044 pp—equivalent to about 36,000 fewer and 72,000 more unemployed workers, respectively, when evaluated using 2019 labor force levels. As a consequence of this "horse race" between harsher summers and milder winters, the annual net effect of climate change has turned positive: roughly 30,000 additional unemployed workers, evaluated at 2019 (Figure A-12).

Guided by Figure 2, we hypothesize that harsher summers and milder winters may help explain the declining volatility in NSA unemployment by raising the floor and lowering the ceiling, respectively. We then assess how much climate change accounts for the decline in monthly NSA unemployment fluctuations. Running the same exercise, we compute that the climate change since the 1950s–70s explains 5.6% of the shrinking variance of the NSA unemployment rate over 2000–2019 (see Figure A-11 for robustness).[19]

As Figure 4b illustrates, the unemployment-augmenting impacts of hot days accelerate over time, whereas the unemployment-reducing effects from fewer cold days remain limited; by the 2010s, even in Q1, these benefits were nearly offset by hot days. Consistently, we find little evidence of dynamic acclimatization (Table A-7). Looking ahead, projections of global warming (IPCC (2023)) suggest that summer unemployment will continue to rise, potentially reversing the long-run moderation in seasonality and amplifying unemployment volatility.[20]

[17]Natural disasters are known to trigger unemployment, as documented in labor market studies of hurricanes (Groen and Polivka (2008); Belasen and Polachek (2008)) and tornadoes (Riesing (2018)).

[18]When aggregate nationwide, rainy days conditional on extreme temperature days consistently explains roughly 6% of NSA unemployment rate.

[19]Several alternative mechanisms may contribute to the remaining decline in seasonal volatility—including the growing non-seasonal service economy and the diffusion of air conditioning—but uncovering these channels remains an open question.

[20]A pronounced spike in summer unemployment has already been observed in the UK in the new century

Figure 4: Simulated Impacts on Unemployment

(a) Impacts of Extreme Temperatures on the Unemployment Rate (over 1990–2019)

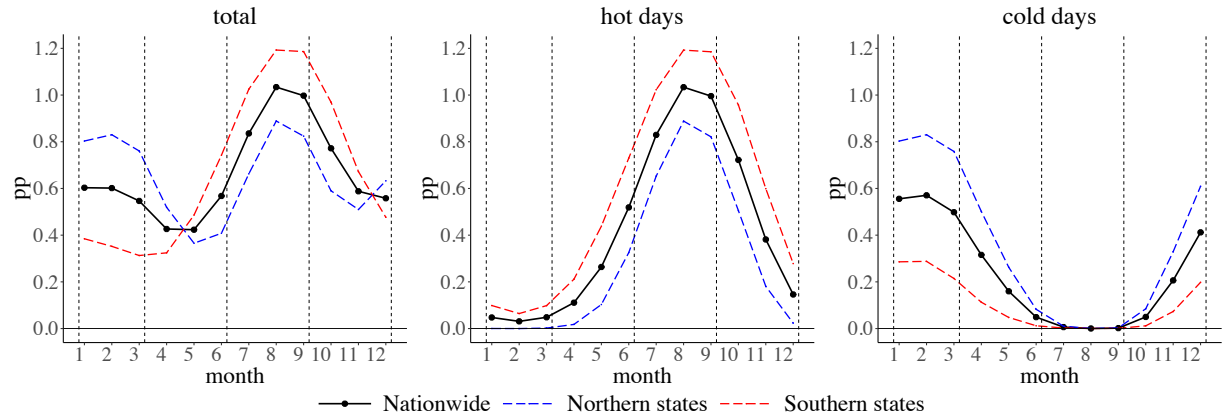

(b) Impacts of Climate Change since the 1950s–70s on the Unemployment Rate

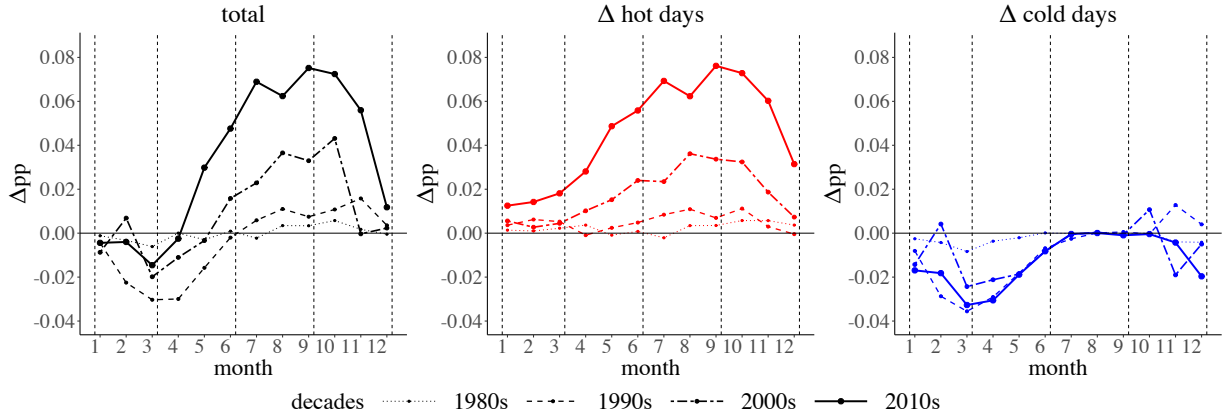

Notes: Simulations are based on a two-tailed model that includes hot days (≥75°F) and cold days (<50°F) with lags of up to two months (Column 3 of Table A-4). An analogously lagged series of rainy days is controlled for, along with county fixed effects and year-month fixed effects. Regressions are weighted by the log of labor force. Panel (a): Monthly exposure to hot days and cold days over 2000–2019 is aggregated using a weighted sum with the vector of lagged coefficients. Southern states include the Southeast (VA, NC, SC, GA, AL, FL), South (TX, LA, MS, AR, OK, KS), Southwest (AZ, NM, UT, CO) and West (CA, NV). Northern states comprise the remaining contiguous U.S. states, including D.C. Panel (b): Period-specific differences in average monthly exposure to hot and cold days relative to 1950–1979 are aggregated using a weighted sum with the vector of lagged coefficients. Decades are defined as 1980–1989 (1980s), 1990–1999 (1990s), 2000–2009 (2000s), and 2010–2019 (2010s).

4 Mechanism

Conceptual framework. To illuminate the channels through which extreme temperatures reshape unemployment dynamics, we outline a conceptual framework. First, on the firm side, weather-sensitive technologies reduce labor efficiency—via fatigue (González-Alonso et al. (1999)), operational errors (Mazloumi et al. (2014)), absenteeism (Somanathan et al. (2021)), and workplace injuries (Park et al. (2021))—and reduce non-labor-related productivity by triggering supply-chain delays (Cachon et al. (2012)), electricity shortages (Adhvaryu et al. (2020)), and machine failures (Garimella and Hughes (2023)). These shocks directly lower labor demand, manifested as fewer vacancy postings and higher layoffs. Second, on the worker side, climate shocks increase thermal discomfort and reservation wages, leading to quits, a small portion of which flow into unemployment (Elsby et al. (2011)). Third, at the labor market level, matching probabilities decline as the market becomes slacker (i.e., vacancies fall relative to unemployment). We investigate these channels through the lens of employment flows below.

Employment flows within counties and sectors. To track climate-induced unemployment inflows and outflows, we examine the dynamics of employment flows. Using the QWI, we study the responses of county-level quarterly job flows across eight sectors (agriculture, mining, construction, manufacturing, transportation, retail, low-skilled service, and high-skilled service) over 1993–2019. Building on the two-tailed specification, Eq.(2), we estimate the following model for county l, sector i, year t, and quarter $q \in \{1, \cdots, 4\}$:

$$\frac{\Delta\ \mathrm{L}_{l,i,t,q}}{\mathrm{E}_{l,i,t,q}} = \beta^h \mathrm{hd}_{l,t,q} + \beta^c \mathrm{cd}_{l,t,q} + \mathbf{\Lambda C}_{l,t,q} + \delta_{l,i} + \delta_{t,q} + \varepsilon_{l,i,t,q}, \tag{3}$$

where the outcome variable is an employment flow, $\Delta\ \mathrm{L}_{l,i,t,q}$, relative to the start-of-quarter employment, $\mathrm{E}_{l,i,t,q}$. $\mathrm{hd}_{l,t,q}$ and $\mathrm{cd}_{l,t,q}$ are hot and cold days per quarter in county l, respectively, and the additional weather variable, $\mathbf{C}_{l,t,q}$, includes rainy days per quarter. The regression is weighted by $\log(\mathrm{E}_{l,i,t,q})$ and standard errors are clustered by state. Given the two-way fixed effects ($\delta_{l,i}$ and $\delta_{t,q}$), β^h and β^c respectively captures the effects of hot and cold days on employment flows, relative to normal (non-hot, non-cold) days.

Table 1a reports the estimates. Column 1 shows that 10 hot days per quarter reduce employment growth by -0.381 percentage points (pp). Consistently, columns 2–3 show that hot days significantly reduce job creation and increase job destruction; however, the contraction in job creation (-0.353 pp) is an order of magnitude larger than the rise in job destruction ($+0.027$

(Figure A-4). A quantitative forecast of future unemployment is beyond the scope of this paper, as it requires a number of assumptions regarding climatic projections, demographic trends and the stability of institutional rules.

Table 1: Extreme Temperature and Quarterly Labor Market Dynamics

(a) Employment Flows at the County-Sector Level (QWI, 1993–2019)

	Dependent variables (percent of start-of-quarter employment (0–100 pp))						
	Emp. Flow	**Job Flow**			**Worker Flow**		
	ΔEmp.	**Creation**	**Destruction**	**Job Turnover** (2) + (3)	**Hires**	**Separations**	**Worker Turnover** (5) + (6)
	(1)	(2)	(3)	(4)	(5)	(6)	(7)
	Descriptive statistics (0–100 pp; mean (sd))						
	2.33	6.35	4.02	10.37	23.2	20.86	44.06
	(4.71)	(5.02)	(1.44)	(5.69)	(12.09)	(9.45)	(21.18)
10 hot days	−0.381	−0.353	0.027	−0.326	−0.327	0.054	−0.272
per quarter	(0.047)	(0.047)	(0.005)	(0.047)	(0.081)	(0.045)	(0.122)
10 cold days	−0.049	−0.104	−0.056	−0.160	−0.423	−0.375	−0.798
per quarter	(0.039)	(0.039)	(0.004)	(0.039)	(0.076)	(0.047)	(0.120)
county × sector FEs	Yes	Yes	Yes	Yes	Yes	Yes	Yes
year × quarter FEs	Yes	Yes	Yes	Yes	Yes	Yes	Yes
Adjusted R^2	0.468	0.513	0.545	0.552	0.573	0.563	0.581

(b) Worker Flows and Matching within States (JOLTS, 2001–2019)

	Dependent variables (percent of end-of-pre-quarter employment (0–100 pp))						
	Worker Flow				**Worker–Firm Matching**		
	Hires	**Separations**			**Job openings**	**Unemploy -ment**	**Market Tightness** (5)/(6)
		Total	**Layoffs**	**Quits**			
	(1)	(2)	(3)	(4)	(5)	(6)	(7)
	Descriptive statistics (0–100 pp; mean (sd))						
	10.62	10.46	4.11	5.61	9.54	6.54	1.75
	(2.10)	(1.86)	(0.81)	(1.31)	(1.58)	(1.38)	(0.53)
10 hot day	−0.214	0.132	0.076	0.058	−0.131	0.039	−0.054
per quarter	(0.086)	(0.034)	(0.017)	(0.021)	(0.053)	(0.021)	(0.017)
10 cold days	−0.101	−0.062	−0.005	−0.057	−0.031	0.061	−0.025
per quarter	(0.071)	(0.030)	(0.015)	(0.017)	(0.036)	(0.018)	(0.011)
state FEs	Yes	Yes	Yes	Yes	Yes	Yes	Yes
year × quarter FEs	Yes	Yes	Yes	Yes	Yes	Yes	Yes
Adjusted R^2	0.880	0.894	0.793	0.904	0.917	0.855	0.835

Notes: Panel (a) $N = 451,647$. Unit of analysis: counties × sectors × years × quarters. Sectors consist of agriculture, mining, construction, manufacturing, transportation, retail, low-skilled service, and high-skilled service. Low-skill services include education, health, leisure and hospitality, and other services. High-skill services include information, business services, finance, and utilities. Eq.(3) is estimated using hot days (≥75°F) and cold days (<50°F). Rainy days per quarter are controlled for. The regressions are weighted by the log of start-of-quarter employment; standard errors clustered by commuting zone. Panel (b) $N = 3,724$. Unit of analysis: states × years × quarters. Eq.(4) is estimated using hot days (≥75°F) and cold days (<50°F). Rainy days per quarter are controlled for. The regressions are weighted by the log of end-of-pre-quarter employment; standard errors are clustered by state.

pp). By contrast, cold days suppress both job creation and destruction. On a net basis, hot and cold days hurt job creation (column 2) and job turnover (column 4). Analogously, Columns 5–6 respectively indicate significantly reduced hires and weakly positive (though statistically insignificant) changes in separations in response to hot days.[21] These results suggest that reduced job creation and hiring increase unemployment by dampening exits from unemployment.

Worker flows within states. We complement the analysis with worker flows obtained from JOLTS, which provides statewide layoffs, job openings, and quits to directly proxy labor demand and supply. Using the JOLTS data from 2001–2019 for 48 states and D.C., we estimate the following counterpart of Eq.(3) for state s in year t and quarter q:

$$\frac{\Delta \mathrm{L}_{s,t,q}}{\mathrm{E}_{s,t,q}} = \beta^h \mathrm{hd}_{s,t,q} + \beta^c \mathrm{cd}_{s,t,q} + \mathbf{\Lambda C}_{s,t,q} + \delta_s + \delta_{t,q} + \varepsilon_{s,t,q}. \tag{4}$$

where the outcome variable is a quarterly worker flow, $\Delta \mathrm{L}_{s,t,q}$, relative to the start-of-quarter employment (proxied by the end-of-previous-quarter employment), $\mathrm{E}_{s,t,q}$, and other notations follow Eq.(3).[22] Columns 1–4 of Table 1b report the results. We find that hot days significantly reduce hires (column 1) and fuel both layoffs and quits (columns 2–4), suggesting that both labor demand and supply shrink in response. Although these worker flows include job-to-job flow and transition to out-of-labor-force, we find that less hires (-0.214 pp), more layoffs ($+0.076$ pp), and quits ($+0.058$ pp) are more likely to contribute to smaller outflows from and larger inflow into unemployment. These results quantitatively suggest that the heat impact primarily operates through the labor demand side. Cold days noticeably decrease both hiring and quits, slowing worker reallocation.

Replacing worker flows $\Delta \mathrm{L}_{s,t,q}$ in the model in Eq.(4) with market-level state variables, columns 5–7 in turn analyze the worker–firm matching. Column 5 shows that hot days reduce job openings, indicating a contraction in labor demand. Driven largely by fewer hires, Column 6 shows that both hot and cold days increase unemployment. Taken together, Column 7 shows that extreme temperatures reduce the labor market tightness, lowering unemployed workers' job-finding probabilities and slowing exits from unemployment.

[21] Job creation/destruction capture establishment-level changes in job positions, whereas hires/separations reflect worker-level flows into and out of jobs (Davis et al. (1996))—when five workers separate and five are hired within the same establishment, job creation and destruction remain zero. See Appendix IV for formal definitions of each proxy.

[22] Analogous to Eq.(3), $\mathbf{C}_{s,t,q}$ includes rainy days per quarter. The regression is weighted by $\log(\mathrm{E}_{s,t,q})$ and standard errors are clustered by state.

5 Consequences for Unemployment Insurance

Established in the aftermath of the Great Depression in the 1930s, the U.S. unemployment insurance (UI) system has provided roughly 50% wage replacement for around 26 weeks for the eligible unemployed workers, where its benefit generosity—covering eligibility, replacement ratio, monitoring rules, and maximum duration—is regulated primarily at the state level.[23] The UI program constitutes a sizable fiscal system, with annual expenditures of $30 billion, surpassing those of federal safety-net programs such as Temporary Assistance to Needy Families (TANF) and Food Stamps. Tracking the climate sensitivity of UI recipiency is not only valuable for quantifying the fiscal externalities of unemployment, but it is also informative about the mechanism of climate-damaged labor demand, given that UI receipt begins with job losses that are through "no fault of their own".

This section estimates the climate effects on UI recipiency across states, and examines the nationwide implications of climate change. We construct the statewide monthly insured unemployment rate, $\text{InsuredUnempRate}_{s,t,m}$, in state s, year t, and month m, defined as UI receipts divided by UI-covered employment (see e.g., FRED). The data are drawn from the administrative UI records over 1990–2019, provided by the Employment and Training Administration (ETA) of the U.S. Department of Labor. We estimate the following model:

$$\text{InsuredUnempRate}_{s,t,m} = \beta^h \text{hd}_{s,t,m} + \beta^c \text{cd}_{s,t,m} + \mathbf{\Lambda C}_{s,t,m} + \delta_s + \delta_{t,m} + \varepsilon_{s,t,m}, \tag{5}$$

where notations follow the previous models, Eq.(1)–(4); for example, $\mathbf{C}_{s,t,m}$ includes rainy days. The regression is weighted by the logarithm of monthly UI-covered employment, and standard errors are clustered by state.

We find that key temperature estimates are both precisely estimated as $\beta^h = 0.105$ (s.e. 0.034) and $\beta^c = 0.292$ (s.e. 0.027). This implies that additional 10 hot days per month increase the insured unemployment rate by 0.11 percentage points (pp), while 10 cold days increase it by 0.29 pp (relative to a mean of 2.28%). We also find analogously significant effects for claimed weeks, compensated weeks and total benefits paid (Table A-8). The estimates are strongly robust to replacing state fixed effects, δ_s, with state-year fixed effects, $\delta_{s,t}$, suggesting that UI extensions or relaxed eligibility triggered by regional unemployment rates are less likely to confound the estimates. Given that UI eligibility requires involuntary job loss, the findings are consistent with a contraction in labor demand, as suggested earlier in Table 1.

Notably, the sensitivities of UI-related outcomes with cold days are broadly three to five times larger than those with hot days (Table A-8), whereas the corresponding estimates for

[23] For background on cross-state unemployment insurance (UI) institutions, see e.g., Nicholson and Needels (2006), Auray et al. (2019) and Rujiwattanapong (2024).

unemployment rates are nearly identical (Table A-1). Albeit partially speculative, we offer two complementary explanations. First, summer unemployment disproportionately reflects seasonal job losses among part-time and lower-earning workers (e.g., construction laborers)—who are less likely to be UI-eligible or receive generous benefits—whereas winter unemployment more often arises from the nonrenewal of annual contracts among full-time, higher-earning workers (e.g., business professionals). Consistent with this pattern, insured unemployment exhibits a much sharper spike from November to January than from June to August (Figure A-13b).

Second, although identification relies on within-state variation, the hot- and cold-day coefficients are primarily informed by geographically distinct sets of states. The UI responses to cold days are driven by Northern states with more generous UI systems (e.g., New Jersey, Massachusetts). By contrast, the identification of the hot-day effects relies disproportionately on Southern states where UI responses are attenuated under less generous benefit regimes (e.g., Florida, Arizona) (Figure A-13a).

Analogous to the earlier quantitative exercise for unemployment (Section 3.2), we next quantify how climate exposure and its long-run change have shaped insured unemployment, allowing for up to two months of lagged effects. Reflecting greater UI sensitivity to cold days, the impacts are concentrated in the fall and winter (Q4/Q1) and generally larger in Northern states than in Southern states (Figure A-14a)—revealing opposing temperature sensitivities that shape unemployment and UI dynamics (recall Figure 4a).

Overall, we find that the temperature warming since the 1950s–70s has reduced insured unemployment over 2000–2019 through milder winters, while increasing it through harsher summers. As these opposing forces counteract each other, the net impact of climate change is close to zero (Figure A-14b). However, UI-augmenting summer effects have expanded more rapidly than winter-related reductions. Taken together, the projected warming is therefore likely to raise insured unemployment—and the associated fiscal burden—through intensifying summer unemployment.

6 Conclusion

Since the pre-industrial era, economic activities have been hampered by the lottery of Mother Nature, including droughts, floods, and the pandemic (Diamond (1999)). Despite its dominant role of within-year fluctuation and real-world implications, little is known about unadjusted high-frequency unemployment dynamics, partly because they are routinely subjected to seasonal adjustment. Using a newly created panel dataset of the U.S. counties, we show that unemployment rates are highly responsive to climate shocks that vary across time and space,

operating primarily through reduced hiring. Aggregating these spatial impacts, our analysis yields a macroeconomic implication of climate change for the secular decline in labor market dynamism.

In light of forecasts of accelerated warming, our findings suggest that summer unemployment is likely to continue rising—an emerging dynamic that cannot be inferred from the standard seasonally-adjusted statistics. In the short run, these forecasts call for strengthened job security measures, targeted in the summer,[24] including UI extensions, public jobs under climate-controlled environments (e.g., Summer Youth Employment Program (Gelber et al. (2016))), and liquidity support to prevent layoffs in heat-exposed industries. In the long run, continued technological development (e.g., air conditioning) will be essential to shield workers from worsening heat shocks (Hötte and Jee (2022)).

We also encourage forecasters to explicitly incorporate weather forecasts into simulation models to improve predictions of unemployment and employment outcomes, especially when heat waves or droughts can be forecast with reasonable accuracy. While summer unemployment is projected to rise in the coming decades, heightened climate risk associated with unprecedented events (e.g., hurricanes, arctic blasts, wildfires) may further amplify unemployment risk. We leave the role of rising climate uncertainty for future work.

[24] In the ancient Egypt, summer flooding of the Nile River created an abundance of unemployed workers. Some historians argue that the kingdom provided pyramid construction as a form of job security (Butzer (1976)).

References

Acemoglu, Daron and Pascual Restrepo, "Robots and Jobs: Evidence from US Labor Markets," *Journal of Political Economy*, 2020, *128* (6), 2188–2244.

Acharya, Viral V, Abhishek Bhardwaj, and Tuomas Tomunen, "Do Firms Mitigate Climate Impact on Employment? Evidence from US Heat Shocks," Working Paper 31967, National Bureau of Economic Research December 2023.

Adhvaryu, Achyuta, Namrata Kala, and Anant Nyshadham, "The light and the heat: Productivity co-benefits of energy-saving technology," *Review of Economics and Statistics*, 2020, *102* (4), 779–792.

Auray, Stéphane, David L. Fuller, and Damba Lkhagvasuren, "Unemployment insurance take-up rates in an equilibrium search model," *European Economic Review*, 2 2019, *112*, 1–31.

Autor, David H., David Dorn, and Gordon H. Hanson, "The China Syndrome: Local Labor Market Effects of Import Competition in the United States," *American Economic Review*, October 2013, *103* (6), 2121–68.

Barreca, Alan, Karen Clay, Olivier Deschenes, Michael Greenstone, and Joseph S Shapiro, "Adapting to Climate Change: The Remarkable Decline in the US Temperature-mortality relationship over the Twentieth Century," *Journal of Political Economy*, 2016, *124* (1), 105–159.

Barsky, Robert B. and Jeffrey A. Miron, "The Seasonal Cycle and the Business Cycle," *Journal of Political Economy*, 1989, *97* (3), 503–534.

Beaulieu, J. Joseph and Jeffrey A. Miron, "A Cross Country Comparison of Seasonal Cycles and Business Cycles," *Economic Journal*, 1992, *102* (413), 772–788.

Belasen, Ariel R and Solomon W Polachek, "How hurricanes affect wages and employment in local labor markets," *American Economic Review*, 2008, *98* (2), 49–53.

Beveridge, William Henry, *Causes and Cures of Unemployment*, London: Longmans, Green and Co., 1931. Based on six radio talks delivered May–June 1931.

Bilal, Adrien and James H. Stock, "A Guide to Macroeconomics and Climate Change," NBER Working Paper 33567, National Bureau of Economic Research 2025.

Black, Dan, Terra McKinnish, and Seth Sanders, "The economic impact of the coal boom and bust," *The Economic Journal*, 2005, *115* (503), 449–476.

Borg, David N., George Havenith, Shane K. Maloney, Yan Hong, and Ollie Jay, "Occupational heat stress and economic burden: A review of global evidence," *The Lancet Planetary Health*, 2021, *5* (8), e572–e581.

Butzer, Karl W., *Early Hydraulic Civilizations in Egypt: A Comparative Perspective*, Chicago: University of Chicago Press, 1976.

Cachon, Gerard P, Santiago Gallino, and Marcelo Olivares, "Severe Weather and Automobile Assembly Productivity," Technical Report 2012.

Chen, Xiaoguang and Lu Yang, "Temperature and Industrial Output: Firm-level Evidence from China," *Journal of Environmental Economics and Management*, 2019, *95*, 257–274.

Chodorow-Reich, Gabriel, John Coglianese, and Loukas Karabarbounis, "The macro effects of unemployment benefit extensions: a measurement error approach," *The Quarterly Journal of Economics*, 2019, *134* (1), 227–279.

Coglianese, John M and Brendan M Price, "Income in the off-season: Household adaptation to yearly work interruptions," *Industrial & Labor Relations Review*, 2025.

Colacito, Riccardo, Bridget Hoffmann, and Toan Phan, "Temperature and Growth: A Panel Analysis of the United States," *Journal of Money, Credit and Banking*, 2019, *51* (2-3), 313–368.

Davis, Steven J., John C. Haltiwanger, and Scott Schuh, *Job Creation and Job Destruction*, Cambridge, MA: MIT Press, 1996.

Dell, Melissa, Benjamin F Jones, and Benjamin A Olken, "Temperature Shocks and Economic Growth: Evidence from the Last Half Century," *American Economic Journal: Macroeconomics*, 2012, *4* (3), 66–95.

_ , _ , and _ , "What Do We Learn from the Weather? The New Climate-Economy Literature," *Journal of Economic Literature*, 2014, *52* (3), 740–98.

Deryugina, Tatyana and Solomon M Hsiang, "Does the Environment Still Matter? Daily Temperature and Income in the United States," Technical Report, National Bureau of Economic Research 2014.

Diamond, Jared, *Guns, Germs, and Steel: The Fates of Human Societies*, New York: W. W. Norton & Company, 1999.

Eliason, Marcus and Donald Storrie, "Job loss is bad for your health–Swedish evidence on cause-specific hospitalization following involuntary job loss," *Social science & medicine*, 2009, *68* (8), 1396–1406.

Elsby, Michael WL, Bart Hobijn, Ayşegül Şahin, Robert G Valletta, Betsey Stevenson, and Andrew Langan, "The Labor Market in the Great Recession—an update to September 2011 [with comment and discussion]," *Brookings Papers on Economic Activity*, 2011, pp. 353–384.

Furceri, Davide, Swarnali A Hannan, Jonathan D Ostry, and Andrew K Rose, "Macroeconomic consequences of tariffs," Technical Report, National Bureau of Economic Research 2018.

Galí, Jordi and Luca Gambetti, "On the sources of the great moderation," *American Economic Journal: Macroeconomics*, 2009, *1* (1), 26–57.

Garimella, Suresh V. and Matt Hughes, "Physicists Explain How Heat Kills Machines and Electronics," *Scientific American*, September 5 2023.

Gathmann, Christina, Ines Helm, and Uta Schönberg, "Spillover effects of mass layoffs," *Journal of the European Economic Association*, 2020, *18* (1), 427–468.

Gelber, Alexander, Adam Isen, and Judd B Kessler, "The effects of youth employment: Evidence from New York City lotteries," *The Quarterly Journal of Economics*, 2016, *131* (1), 423–460.

Geremew, Menelik and François Gourio, "Seasonal and Business Cycles of U.S. Employment," *Economic Perspectives, Federal Reserve Bank of Chicago*, 2018, *42* (3), 1–28.

González-Alonso, José, Christina Teller, Signe L Andersen, Frank B Jensen, Tino Hyldig, and Bodil Nielsen, "Influence of body temperature on the development of fatigue during prolonged exercise in the heat," *Journal of applied physiology*, 1999, *86* (3), 1032–1039.

Groen, Jeffrey A and Anne E Polivka, "The effect of Hurricane Katrina on the labor market outcomes of evacuees," *American Economic Review*, 2008, *98* (2), 43–48.

Gruber, Jonathan, "The Consumption Smoothing Benefits of Unemployment Insurance," *American Economic Review*, 1997, *87* (1), 192–205.

Hancock, Peter A, Jennifer M Ross, and James L Szalma, "A meta-analysis of performance response under thermal stressors," *Human factors*, 2007, *49* (5), 851–877.

Hodrick, Robert J and Edward C Prescott, "Postwar US business cycles: an empirical investigation," *Journal of Money, credit, and Banking*, 1997, pp. 1–16.

Hötte, Kerstin and Su Jung Jee, "Knowledge for a warmer world: A patent analysis of climate change adaptation technologies," *Technological Forecasting and Social Change*, 2022, *183*, 121879.

IPCC, *Climate Change 2023: Synthesis Report*, Geneva, Switzerland: Intergovernmental Panel on Climate Change, 2023. Contribution of Working Groups I, II and III to the Sixth Assessment Report of the Intergovernmental Panel on Climate Change.

Ireland, Andrew, David Johnston, and Rachel Knott, "Impacts of Extreme Heat on Labor Force Dynamics," 2025. Revise and Resubmit, Journal of Labor Economics.

Kim, Hee Soo, Christian Matthes, and Toàn Phan, "Severe Weather and the Macroeconomy," *American Economic Journal: Macroeconomics*, April 2025, *17* (2), 315–41.

Kim, Ryan and Jonathan Vogel, "Trade shocks and labor market adjustment," *American Economic Review: Insights*, 2021, *3* (1), 115–130.

Lai, Wangyang, Yun Qiu, Qu Tang, Chen Xi, and Peng Zhang, "The Effects of Temperature on Labor Productivity," *Annual Review of Resource Economics*, 2023, *15* (1), 213–232.

Ma, Enjie (Jack), "Extreme Heat and Directed Innovation," 2025. Job Market Paper, Cornell University,
urlhttps://enjiema.com/files/JackMa$_JMP.pdf$.

Mazloumi, Adel, Farideh Golbabaei, Somayeh Mahmood Khani, Zeinab Kazemi, Mostafa Hosseini, Marzieh Abbasinia, and Somayeh Farhang Dehghan, "Evaluating effects of heat stress on cognitive function among workers in a hot industry," *Health promotion perspectives*, 2014, *4* (2), 240.

Milner, Allison, Andrew Page, and Anthony D LaMontagne, "Long-term Unemployment and Suicide: A Systematic Review and Meta-analysis," *PloS One*, 2013, *8* (1), e51333.

Nicholson, Walter and Karen Needels, "Unemployment insurance: Strengthening the relationship between theory and policy," *Journal of Economic Perspectives*, 2006, *20* (3), 47–70.

Park, Jisung, Nora Pankratz, and Arnold Behrer, "Temperature, Workplace Safety, and Labor Market Inequality," Technical Report 2021.

Ponticelli, Jacopo, Qiping Xu, and Stefan Zeume, "Temperature and Local Industry Concentration," Working Paper 31533, National Bureau of Economic Research August 2023.

Price, Brendan M. and Melanie Wasserman, "The Summer Drop in Female Employment," *The Review of Economics and Statistics*, 06 2024, pp. 1–46.

Qiu, Xincheng and Masahiro Yoshida, "Climate Change and the Decline of Labor Share," Technical Report, IZA Discussion Papers 2024.

Raphael, Steven and Rudolf Winter-Ebmer, "Identifying the Effect of Unemployment on Crime," *The Journal of Law and Economics*, 2001, *44* (1), 259–283.

Riesing, Kara, "Effect of Tornadoes on Local Labor Markets," Technical Report, working paper 2018.

Rujiwattanapong, W. Similan, "Job Search, Job Findings and the Role of Unemployment Insurance History," Discussion Papers 2441, Centre for Macroeconomics (CFM) Sep 2024.

_ , "Unemployment dynamics and endogenous unemployment insurance extensions," *European Economic Review*, 2025, *178*, 105106.

_ **and Masahiro Yoshida**, "Climate Change and Unemployment Seasonality: Evidence from U.S. Counties," WINPEC Working Paper E2512, Waseda Institute of Political Economy (WINPEC) 5 2025.

Somanathan, Eswaran, Rohini Somanathan, Anant Sudarshan, and Meenu Tewari, "The Impact of Temperature on Productivity and Labor Supply: Evidence from Indian Manufacturing," *Journal of Political Economy*, 2021, *129* (6), 1797–1827.

Stock, James H and Mark W Watson, "Business cycle fluctuations in US macroeconomic time series," *Handbook of macroeconomics*, 1999, *1*, 3–64.

Xiao, Zhanbing, "Labor Exposure to Climate Risk, Productivity Loss, and Capital Deepening," 2021. Working paper, posted 1 August 2021; revised 29 March 2024.

Yoshida, Masahiro, "Climate Change and the Rise of Adult Male Dropouts," *SSRN working paper*, 2025.

Zhang, Peng, Olivier Deschenes, Kyle Meng, and Junjie Zhang, "Temperature Effects on Productivity and Factor Reallocation: Evidence from a Half Million Chinese Manufacturing Plants," *Journal of Environmental Economics and Management*, 2018, *88*, 1–17.

Zivin, Joshua Graff and Matthew Neidell, "Temperature and the Allocation of Time: Implications for Climate Change," *Journal of Labor Economics*, 2014, *32* (1), 1–26.

APPENDICES FOR ONLINE PUBLICATION

Climate Change and Unemployment Dynamics: Evidence from U.S. Counties

W. Similan Rujiwattanapong and Masahiro Yoshida

February, 2026

I Appendix: Data

I.1 Climate Change

Weather stations. Panel (a) of Figure A-1 shows the long-run trend in the number of weather stations operating in the U.S. from 1900 to 2019, separated by the availability of stations' daily records in each year (four series). The number of stations in operation generally increases over time. Daily weather measures are constructed using only stations with complete daily records in each year. Panel (b) of Figure A-1 illustrates the spatial distribution of stations with complete records (red dots) in 2019 overlaid on county boundaries. The map shows dense climate monitoring overall, particularly in populous areas.

Figure A-1: Weather Stations in the U.S. Mainland

(a) Number of Operating Stations (1900–2019)

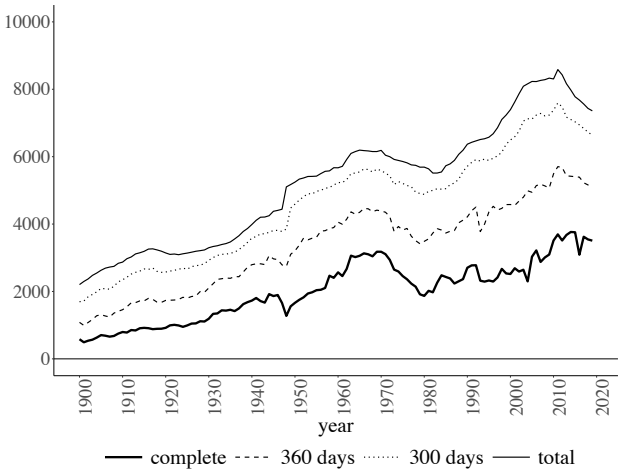

(b) Spatial Distribution (2019)

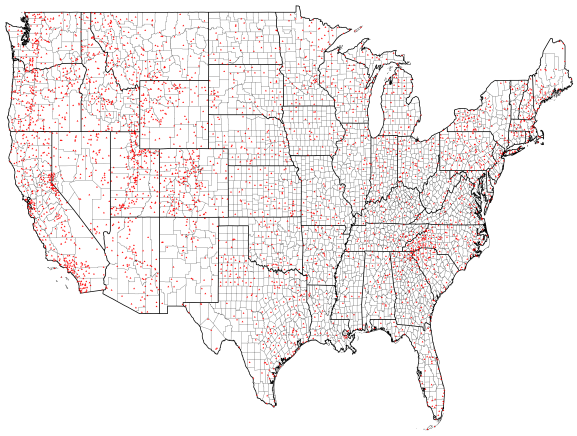

Notes: Panel (a): the number of weather stations in the U.S. mainland from the Global Historical Climatology Network Daily (GHCN-daily), provided by the National Climatic Data Center (NCDC) of the National Oceanic and Atmospheric Administration (NOAA). Panel (b): the distribution of weather stations with complete records (red dots) over county borders (thin lines) and state borders (thick lines).

Weather variables at the county level. We construct daily minimum and maximum temperatures, precipitation, and snowfall from GHCN-Daily stations with complete daily records in each year, 1950–2019. Following the inverse-distance weighting approach commonly used in the literature, we compute county-level daily weather measures by averaging observations from the three weather stations closest to each county's 2020 population centroid (as provided by the Census Bureau), with weights given by the inverse distance to the centroid.

Figure A-2 displays the geographic distribution of hot and cold days across counties. Panel (a1/b1) shows the annual frequency of hot days and cold days averaged over the period 2000–2019, and Panel (a2/b2) illustrates the change in period-averaged exposure to hot and cold days between 1950–1979 and 2000–2019.

Figure A-2: Extreme Temperature Days across U.S. Counties

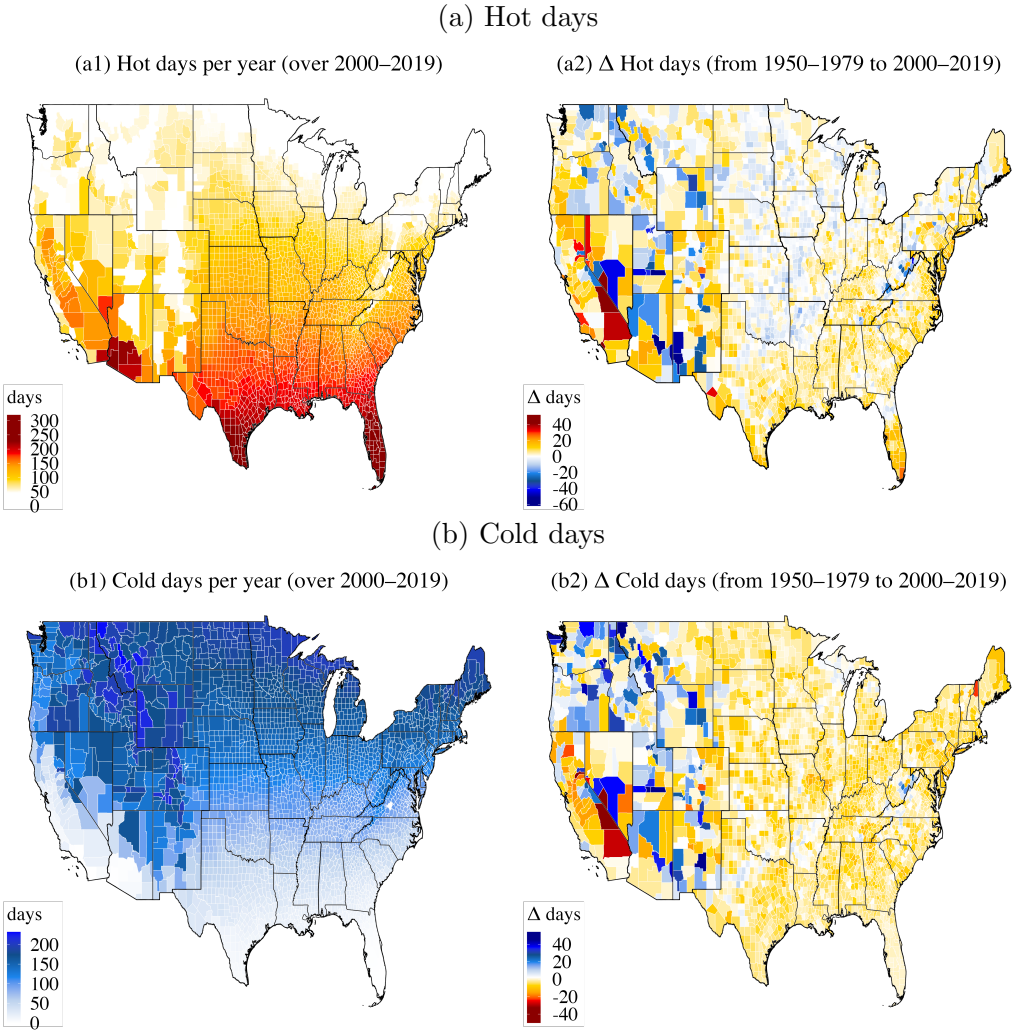

Notes: Panel (a1/b1): Period-average exposure over 2000–2019. Panel (a2/b2): Changes in period-average exposure between 1950–1979 and 2000–2019. Thresholds for hot and cold days are set to 75°F and 50°F, respectively, based on average working-hour temperature, constructed as a weighted average of daily maximum and minimum temperatures, with a weight of 0.75 on the maximum.

Precipitation. Figure A-3 shows the spatial distribution of precipitation across counties over the period 2000–2019, as well as the change in period-averaged exposure to rainy days between 1950–1979 and 2000–2019.

Figure A-3: Precipitation across U.S. Counties

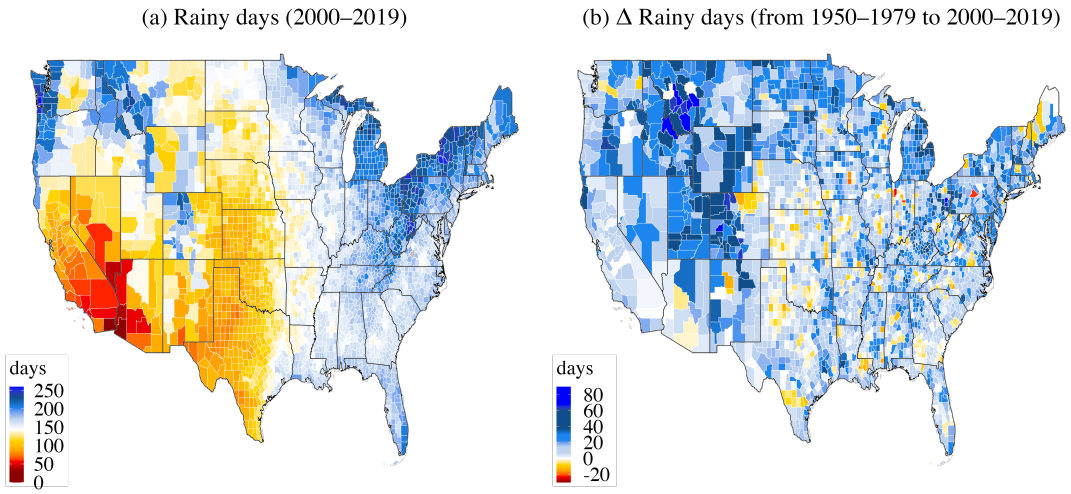

Notes: Panel (a): Period-averaged exposure over 2000–2019. Panel (b): Changes in period-averaged exposure between 1950–1979 and 2000–2019.

Humidity. The relative humidity is constructed from dew points at another set of station records from NOAA's Global Summary of the Day (GSoD). To compute a relative humidity, we use a standard meteorological formula from Glossary of Meteorology by the American Meteorological Society. A relative humidity H_d of a day d and a vapor pressure $v(T)$ as a function of temperature T is given by:

$$H_d \equiv \frac{v(T_{dew})}{v(T_d)}; v(T) = 0.6112 \exp(17.67T/(T + 243.5)) \times 10 \tag{A1}$$

where $v(T_{dew})$ is a saturation vapor pressure at the dew point T_{dew} and $v(T_d)$ is a day d 's vapor pressure at a temperature T_d. Heat Index$_d$ of a day d is a function of a temperature T_d and a daily relative humidity H_d such that

$$\text{Heat Index}_d = 0.81T + H_d(0.99T_d - 14.3) + 46.3. \tag{A2}$$

I.2 Unemployment

Unemployment seasonality outside the U.S. Figure A-4 illustrates changes in seasonal unemployment rates outside the U.S., focusing on Canada, Germany, the UK, and the OECD aggregate. Canada, Germany, and the OECD have experienced a decline in seasonal volatility similar to that in the U.S. By contrast, seasonality in the UK has been amplified by rising summer unemployment.

Figure A-4: The Dynamics of Seasonal Unemployment Rates across Countries

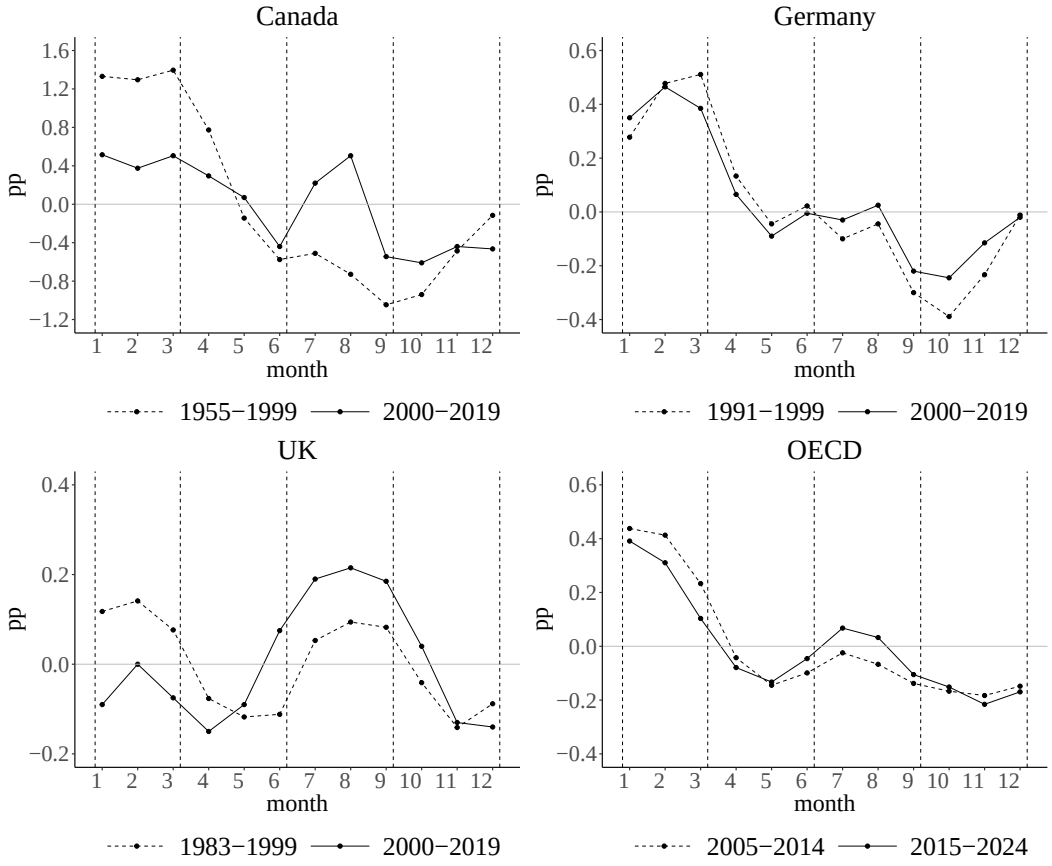

Notes: In each period, a seasonal unemployment rate is computed as the difference between period-average NSA and SA monthly nationwide (or OECE-wide) unemployment rates, as provided by the FRED (Federal Reserve Economic Data).

Seasonal unemployment dynamics across commuting zones. As a commuting-zone counterpart to Figure 2c, Figure A-5 shows that half-year exposure to hot days in summer and cold days in winter is positively associated with changes in seasonal unemployment across commuting zones over 1990–2019.

Figure A-5: Temperature Shocks and Seasonal Unemployment Rate Swings

(ΔNSA unemployment rate within commuting zones averaged over 1990–2019)

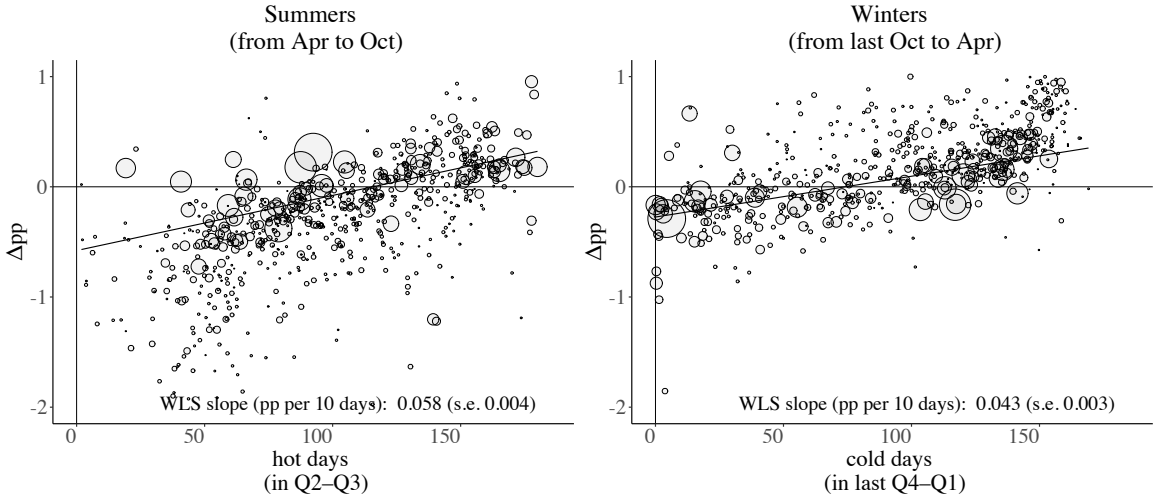

Notes: County-level exposure to hot days (≥75°F) and cold days (<50°F) is aggregated to the commuting zone (CZ) level, weighted by county-level labor force over 1990–2019. The half-year seasonal swing in unemployment rate in CZs are computed from the BLS monthly data. The fitted lines are weighted by period-average labor force, represented by the bubble size. The y-axis is truncated at ˇ2 for visibility.

The seasonal regularity in employment. In contrast to the seasonality of unemployment, Figure A-6 documents the seasonality of employment. Figure A-6a shows moderation in the seasonal employment rate (i.e., the employment-to-population ratio). Figure A-6b indicates that hotter summers and colder winters are associated with slower employment growth and larger declines within states, respectively.

Figure A-6: Employment Seasonality in the U.S.

(a) Long-run Trend of Seasonal Employment Rate

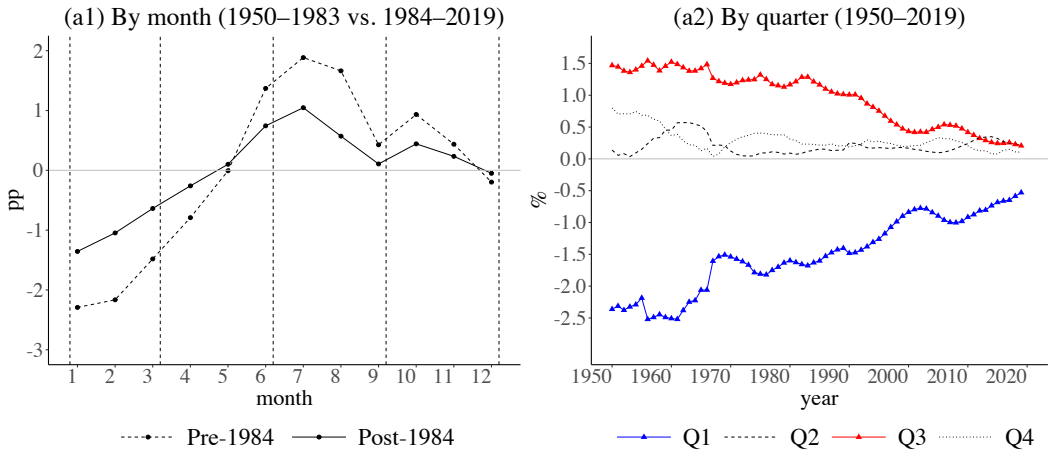

(b) Temperature Shocks and Seasonal Employment Rate Swings

(ΔNSA employment rate within states averaged over 1990–2019)

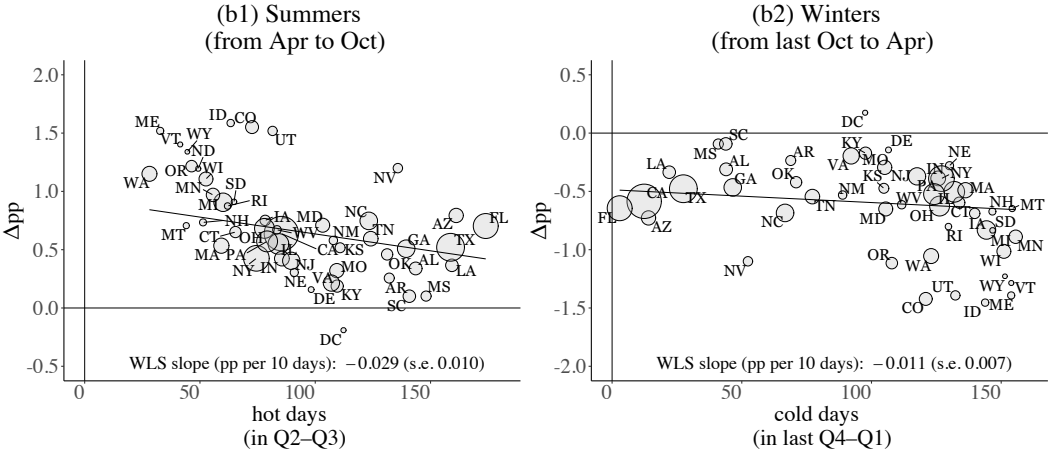

Notes: Panel (a): Within a given month or quarter, the seasonal employment rate is defined as the difference between the non-seasonally adjusted (NSA) and seasonally adjusted (SA) nationwide employment-to-population ratios, computed using BLS employment series (ages 16+) and SEER working-age population data (ages 15+). Panel (a1): Change in the period-averaged seasonal monthly employment rate, comparing 1950–1983 with 1984–2019. Panel (a2): Five-year moving average of the quarterly seasonal employment rate. Panel (b): County-level exposure to analogously defined hot and cold days is aggregated to states plus D.C. averaged during 1990–2019, weighted by county labor force. The fitted lines are weighted by the period-average population (ages 15+), represented by bubble size.

II Appendix: Empirical Analysis

II.1 Robustness

Fixed effects. Figure A-7 tests the sensitivity of our baseline temperature estimates with county fixed effects (FEs) and year-month FEs (thin black lines) to alternative FE combinations.

Figure A-7: Robustness to Fixed Effects (FEs)

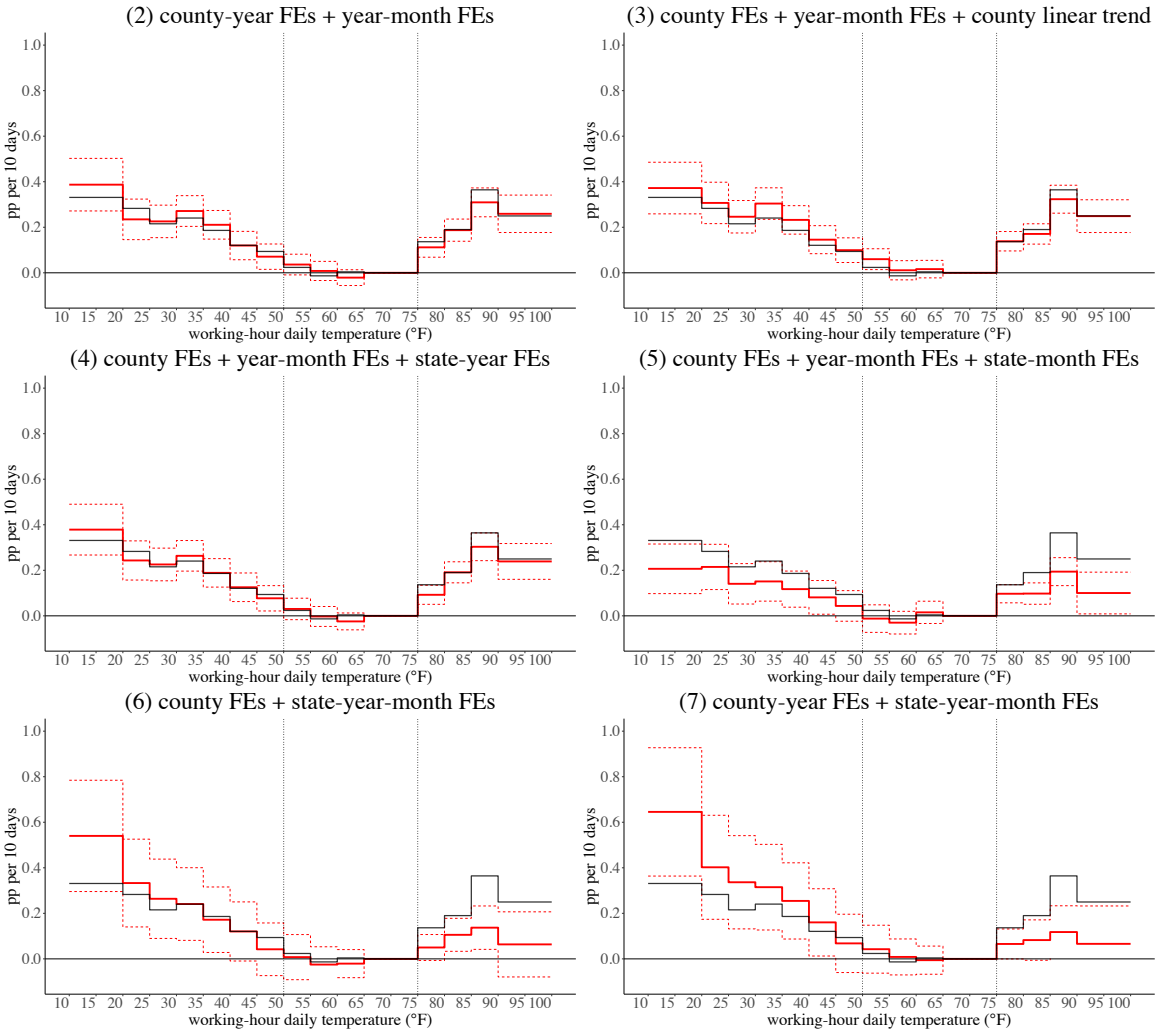

Notes: Effects of temperature exposure on unemployment rate (pp, 1990–2019): 10 days in each temperature bin (relative to 65–75°F). $N = 1,117,358$. Unit of analysis: counties × years × months. In Eq.(1), county FEs and year-month FEs are replaced with alternative combinations of FEs in panels (2)–(7), corresponding to the columns reported in Table A-2. Rainy days per month are controlled. Regressions are weighted by the log of labor force. Dotted red lines are 95% confidence intervals, constructed from standard errors clustered by commuting zone.

Additional weather variables. Figure A-8 tests the robustness to inclusion of additional weather controls. Including or excluding these weather variables does not significantly alter the temperature estimates.

Figure A-8: Robustness to Additional Weather Controls

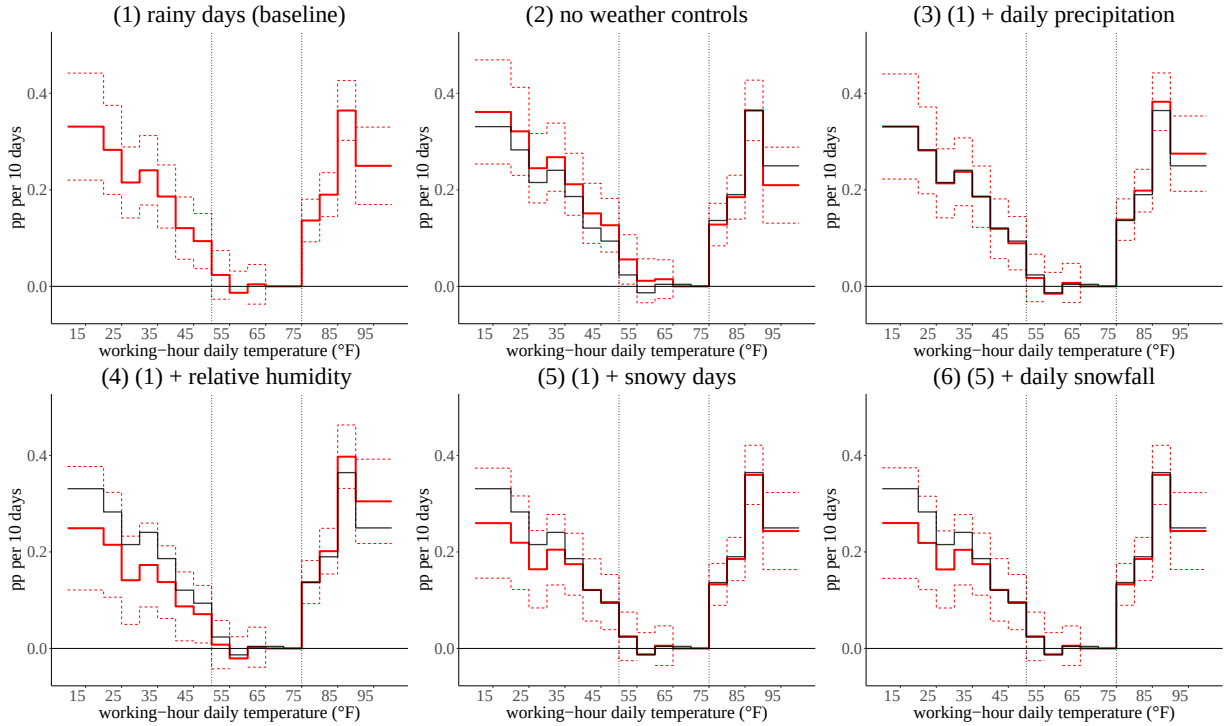

Notes: Effects of temperature exposure on unemployment rate (pp, 1990–2019): 10 days in each temperature bin (relative to 65–75°F). $N = 1,117,358$. Unit of analysis: counties × years × months. Eq.(1) is estimated with alternative additional weather variables $\mathbf{C}_{l,t,m}$ in (2)–(6). Note that (1)–(6) corresponds with columns in Table A-3. County fixed effects and year-month fixed effects are controlled for. Regressions are weighted by the log of labor force. Red dotted lines are 95% confidence intervals, constructed from standard errors clustered by commuting zone. Thin black lines indicate point estimates of the baseline (1).

Two-tailed models under alternative temperature cutoffs. We simplify treatment variables $\sum_{b\in\{1,\cdots,10,13,\cdots,16\}} \text{days}^b_{l,t,m}$ in the baseline model into two summary measures, as follows:

$$\text{UnempRate}_{l,t,m} = \beta^h \text{hd}_{l,t,m} + \beta^c \text{cd}_{l,t,m} + \mathbf{\Lambda C}_{l,t,m} + \delta_l + \delta_{t,m} + \varepsilon_{l,t,m}, \tag{A3}$$

where $\text{hd}_{l,t,m}$ and $\text{cd}_{l,t,m}$ denote hot days ($\geq$75°F) and cold days ($<$50°F), respectively. Alternatively, Table A-1 tests reasonable pairs of temperature cutoffs for hot and cold days. Consistent with the U-shape estimates at Figure 3a1, columns 1–5 in Panel (a) and (b) yield significantly positive effects on NSA unemployment rates. By contrast, temperature effects on SA unemployment rates are an order of magnitude smaller and, for cold days, are mostly imprecisely

estimated and difficult to interpret.

Table A-1: Robustness to Temperature Cutoffs (Two-Tailed Models, 1990–2019)

	Panel (a): Cutoffs for Hot Days					
		Baseline				
	73°F	75°F	77°F	80°F	85°F	90°F
	Dependent variable: NSA unemployment rate (pp)					
	(1)	(2)	(3)	(4)	(5)	(6)
10 hot days	0.201	0.240	0.262	0.259	0.201	0.093
	(0.025)	(0.026)	(0.024)	(0.022)	(0.020)	(0.029)
10 cold days (<50°F)	0.288	0.248	0.215	0.206	0.274	0.351
	(0.025)	(0.026)	(0.025)	(0.024)	(0.024)	(0.024)
Adjusted R^2	0.713	0.713	0.714	0.714	0.713	0.713
	Dependent variable: SA unemployment rate (pp)					
	(7)	(8)	(9)	(10)	(11)	(12)
10 hot days	0.009	0.015	0.014	0.011	0.012	−0.018
	(0.007)	(0.008)	(0.008)	(0.008)	(0.009)	(0.014)
10 cold days (<50°F)	0.003	−0.001	−0.002	−0.0004	0.001	0.009
	(0.006)	(0.007)	(0.007)	(0.008)	(0.006)	(0.004)
Adjusted R^2	0.747	0.747	0.747	0.747	0.747	0.747
	Panel (b): Cutoffs for Cold Days					
		Baseline				
	55°F	50°F	45°F	40°F	35°F	30°F
	Dependent variable: NSA unemployment rate (pp)					
	(1)	(2)	(3)	(4)	(5)	(6)
10 hot days (≥75°F)	0.295	0.240	0.220	0.234	0.263	0.293
	(0.026)	(0.026)	(0.023)	(0.022)	(0.022)	(0.022)
10 cold days	0.202	0.248	0.259	0.250	0.239	0.235
	(0.023)	(0.026)	(0.026)	(0.026)	(0.027)	(0.031)
Adjusted R^2	0.713	0.713	0.714	0.713	0.713	0.713
	Dependent variable: SA unemployment rate (pp)					
	(7)	(8)	(9)	(10)	(11)	(12)
10 hot days (≥75°F)	0.016	0.015	0.017	0.018	0.019	0.018
	(0.007)	(0.008)	(0.008)	(0.007)	(0.007)	(0.006)
10 cold days	−0.004	−0.001	−0.005	−0.008	−0.010	−0.013
	(0.006)	(0.007)	(0.006)	(0.006)	(0.006)	(0.006)
Adjusted R^2	0.747	0.747	0.747	0.747	0.747	0.747

Notes: $N = 1,117,358$ for the NSA unemployment rates and $N = 1,114,548$ for the SA series; for some county–year–month cells, seasonal adjustment is not reported by the BLS. Unit of analysis: counties × years × months. The two-tailed model (Eq.(A3)) is estimated using reasonable temperature cutoffs. Rainy days are controlled for, along with county fixed effects and year-month fixed effects. Regressions are weighted by the log of labor force; standard errors clustered by commuting zone.

Robustness to fixed effects: two-tailed models Using the two-tailed model, Table A-2 reports the estimates under alternative fixed-effect combinations corresponding to panels (2)–(7) in Figure A-7, in addition to the baseline specification (1). Adding state-month FEs or state-year-month FEs reduces the estimates by roughly half, but the effects remain precisely estimated.

Table A-2: Robustness to Fixed Effects (Two-Tailed Model, 1990–2019)

	Dependent variable: unemployment rate (pp)						
	Baseline						
	(1)	(2)	(3)	(4)	(5)	(6)	(7)
10 hot days	0.240	0.229	0.219	0.225	0.125	0.132	0.139
	(0.026)	(0.027)	(0.025)	(0.026)	(0.025)	(0.039)	(0.045)
10 cold days	0.248	0.255	0.262	0.254	0.108	0.143	0.151
	(0.026)	(0.027)	(0.026)	(0.026)	(0.029)	(0.049)	(0.053)
				Fixed effects			
county FEs	Yes	-	Yes	Yes	Yes	Yes	-
county-year FEs	-	Yes	-	-	-	-	Yes
county linear trend	-	-	Yes	-	-	-	-
year-month FEs	Yes	Yes	Yes	Yes	Yes	-	-
state-month FEs	-	-	-	-	Yes	-	-
state-year FEs	-	-	-	Yes	-	-	-
state-year-month FEs	-	-	-	-	-	Yes	Yes
Adjusted R^2	0.713	0.904	0.767	0.784	0.721	0.795	0.918

Notes: $N = 1,117,358$. Unit of analysis: counties × years × months. The two-tailed model (Eq.(A3)) is estimated using hot days (≥75°F) and cold days (<50°F) with alternative combination of fixed effects in (2)–(7). Rainy days per month are controlled for. Regressions are weighted by the log of labor force; standard errors clustered by commuting zone.

Robustness to additional weather variables: two-tailed models Table A-3 examines the sensitivity of temperature effects in the simpler two-tailed model to alternative sets of additional weather controls, corresponding to panels (1)–(6) in Figure A-8. Column 1 repeats our two-tailed baseline specification. Column 2 includes no additional weather controls. Columns 3 and 4 add daily precipitation and relative humidity (constructed by Eq.(A1)), respectively, to the baseline. The estimates remain broadly stable across specifications. Columns 5 and 6 sequentially add snowfall on the extensive and intensive margins. The magnitudes of temperature estimates are modestly reduced, but remain precisely estimated. As an extension, Column 7 introduces "uncomfortable days," defined as days with a heat index above 80°F, that interact temperature with relative humidity (constructed by Eq.(A2)) and yields larger and more precise estimates than the baseline hot-day effects.

Table A-3: Robustness to Additional Weather Variables (Two-Tailed Models, 1990-2019)

	Dependent variable: unemployment rate (pp)						
	Baseline						
	(1)	(2)	(3)	(4)	(5)	(6)	(7)
10 hot days	0.240	0.225	0.247	0.243	0.206	0.206	
	(0.026)	(0.025)	(0.025)	(0.026)	(0.024)	(0.024)	
10 uncomfortable days							0.266
							(0.023)
10 cold days	0.248	0.262	0.252	0.219	0.208	0.208	0.197
	(0.026)	(0.026)	(0.024)	(0.029)	(0.025)	(0.025)	(0.026)
10 rainy days	0.151		0.137	0.098	0.145	0.145	0.115
	(0.023)		(0.021)	(0.022)	(0.023)	(0.023)	(0.021)
daily precipitation			0.049				
			(0.012)				
relative humidity ($[0, 100]\%$)				0.007			
				(0.002)			
10 snowy days					0.117	0.119	
					(0.023)	(0.021)	
daily snowfall (10 cm)						−0.004	
						(0.015)	
N	1,117,358	1,117,370	1,110,582	1,117,358	1,117,358	1,117,358	1,117,358
Adjusted R^2	0.713	0.713	0.713	0.714	0.714	0.714	0.714

Notes: Unit of analysis: counties × years × months. The two-tailed model (Eq.(A3)) is estimated using hot days (≥75°F) and cold days (<50°F), along with alternative additional weather variables $\mathbf{C}_{l,t,m}$ in (2)–(6). County fixed effects and year-month fixed effects are controlled for. Regressions are weighted by the log of labor force; standard errors clustered by commuting zone.

Two-tailed models with lagged weather variables. Table A-4 shows the robustness results, adding lagged hot days and cold days in the two-tailed baseline model. Hot days exhibit larger, more persistent, and more precisely estimated lagged effects than cold days.

Table A-4: Robustness to Lagged Weather Variables (Two-Tailed Models, 1990–2019)

	Dependent variable: unemployment rate (pp)					
	Baseline		Simulation baseline			
	(1)	(2)	(3)	(4)	(5)	(6)
10 hot days	0.240	0.110	0.150	0.161	0.161	0.150
	(0.026)	(0.017)	(0.018)	(0.019)	(0.019)	(0.018)
1-month lag		0.248	0.139	0.150	0.151	0.148
		(0.023)	(0.015)	(0.015)	(0.015)	(0.015)
2-month lag			0.168	0.116	0.124	0.122
			(0.020)	(0.015)	(0.015)	(0.015)
3-month lag				0.085	0.077	0.079
				(0.013)	(0.011)	(0.011)
4-month lag					0.005	0.025
					(0.011)	(0.007)
5-month lag						−0.047
						(0.016)
10 cold days	0.248	0.119	0.156	0.159	0.167	0.170
	(0.026)	(0.016)	(0.017)	(0.018)	(0.018)	(0.017)
1-month lag		0.166	0.072	0.083	0.082	0.085
		(0.022)	(0.015)	(0.014)	(0.014)	(0.014)
2-month lag			0.085	0.048	0.051	0.053
			(0.017)	(0.013)	(0.013)	(0.012)
3-month lag				0.030	0.006	0.001
				(0.012)	(0.010)	(0.010)
4-month lag					0.037	0.027
					(0.010)	(0.008)
5-month lag						0.029
						(0.014)
N	1,117,358	1,117,357	1,117,356	1,117,355	1,117,354	1,117,353
Adjusted R^2	0.713	0.716	0.716	0.717	0.717	0.717

Notes: Unit of analysis: counties × years × months. The two-tailed model (Eq.(A3)) is estimated using hot days (≥75°F) and cold days (<50°F) with a M-month distribution of lags ($M \in \{0, \cdots, 5\}$). An analogously lagged series of rainy days is controlled for, along with county fixed effects and year-month fixed effects. Regressions are weighted by the log of labor force; standard errors clustered by commuting zone.

II.2 Auxiliary Analyses

Clustering units. Figure A-9 examines alternative clustering units for standard errors. 95% confidence intervals, constructed using standard errors clustered by commuting zone, by state, and by state-year (two-way clustering), are illustrated separately.

Figure A-9: Robustness to Clustering Units

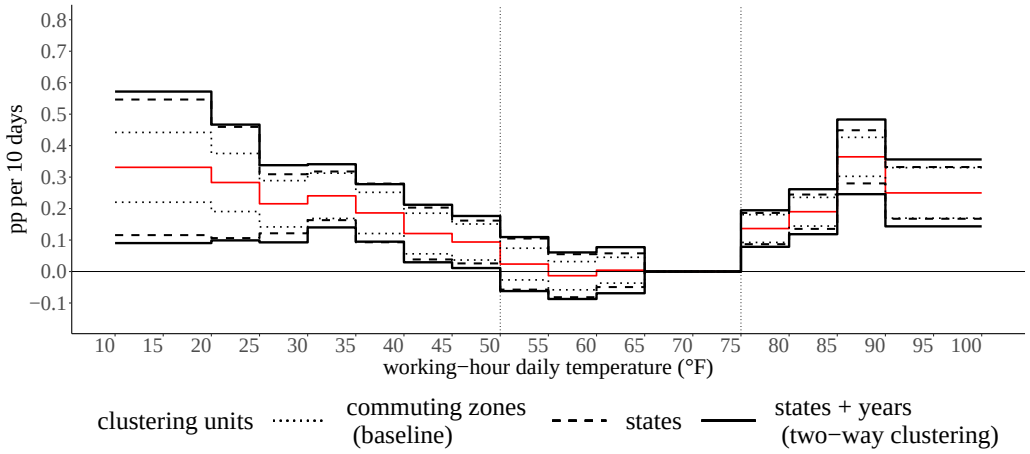

Notes: Effects of temperature exposure on unemployment rate (pp, 1990–2019): 10 days in each temperature bin (relative to 65–75°F). $N = 1,117,358$. Unit of analysis: counties × years × months. Eq.(1) is estimated with alternative units of clustering errors. Rainy days are controlled for, along with county fixed effects and year-month fixed effects. Regressions are weighted by the log of labor force. 95% confidence intervals, constructed from standard errors under alternative clustering units, are illustrated around the point estimates (red lines).

Robustness to moving-average treatment windows. Table A-5 reports the estimates from the the two-tailed baseline model using an M-month ($M \in \{1, \cdots, 6\}$) moving-average treatment window for weather variables.

Table A-5: Robustness to Moving-average Treatment Windows (Two-Tailed Models, 1990–2019)

	Dependent variable: unemployment rate (pp)					
	Moving-average treatment window					
	Baseline 1 month	2 months	3 months	4 months	5 months	6 months
	(1)	(2)	(3)	(4)	(5)	(6)
10 hot days	0.240	0.350	0.450	0.530	0.571	0.568
per month	(0.026)	(0.037)	(0.047)	(0.055)	(0.057)	(0.055)
10 cold days	0.248	0.294	0.314	0.308	0.295	0.272
per month	(0.026)	(0.035)	(0.043)	(0.048)	(0.051)	(0.049)
Adjusted R^2	0.713	0.715	0.716	0.716	0.715	0.713

Notes: $N = 1,117,358$. Unit of analysis: counties × years × months (moving-averaged over an M-month ($M \in \{1, \cdots, 6\}$) treatment window). The two-tailed model (Eq.(A3)) is estimated using M-month moving average of hot days ($\geq$75°F) and cold days ($<$50°F). An M-month moving average of rainy days is controlled for, along with county fixed effects and year-month fixed effects. Regressions are weighted by the log of labor force; standard errors clustered by commuting zone.

Spatial heterogeneity. How does the climate impact differ across space? To see this, we start by allowing temperature effects in the two-tailed model to vary with regional climate normals, proxied by the difference in period-averaged exposure to hot and cold days during the 1980s.

Table A-6 tests heterogeneous impacts across regional climate normals. We find that heat effects are stronger in historically hot regions (e.g., the Southeast), and cold effects are stronger in historically cold regions (e.g., the Northeast). This plausibly reflects their greater exposure to the extreme upper and lower tails of the daily temperature distribution.

Table A-6: Spatial Heterogeneity across Differential Climate Normals (1990–2019)

	Dependent variable: unemployment rate (pp)				
	Cutoffs for cold days				
	Baseline				
	55°F	50°F	45°F	40°F	35°F
	(1)	(2)	(3)	(4)	(5)
10 hot days ($\geq$ 75°F)	0.138	0.120	0.120	0.113	0.093
	(0.020)	(0.020)	(0.020)	(0.021)	(0.024)
10 cold days	0.028	0.079	0.089	0.087	0.092
	(0.022)	(0.026)	(0.026)	(0.023)	(0.022)
10 hot days	0.005	0.005	0.007	0.010	0.013
$\times$ hot days minus cold days (1980s)	(0.001)	(0.001)	(0.001)	(0.001)	(0.001)
10 cold days	−0.013	−0.013	−0.013	−0.014	−0.018
$\times$ hot days minus cold days (1980s)	(0.002)	(0.002)	(0.003)	(0.003)	(0.004)
Adjusted R^2	0.714	0.714	0.714	0.714	0.714

Notes: $N = 1,117,358$. Unit of analysis: counties $\times$ years $\times$ months. The two-tailed model (Eq.(A3)) is estimated using hot days ($\geq$75°F) and cold days under different cutoffs, interacted with a measure of historical climate defined as the 1980s average difference between hot and cold days. Rainy days are controlled for, along with county fixed effects and year-month fixed effects. Regressions are weighted by the log of labor force; standard errors clustered by commuting zone.

Adaptation. Does the climate impact diminish over time, consistent with adaptation? Table A-7 estimates models interacted with linear time trend across different cold-day thresholds. As all the coefficients on the interaction terms are statistically insignificant, we find little evidence of adaptation.

Table A-7: Intertemporal Adaptation (1990–2019)

	Dependent variable: unemployment rate (pp)				
	Cutoffs for cold days				
	Baseline				
	55°F	50°F	45°F	40°F	35°F
	(1)	(2)	(3)	(4)	(5)
10 hot days (≥75°F)	0.354	0.292	0.270	0.284	0.313
	(0.048)	(0.051)	(0.052)	(0.052)	(0.052)
10 cold days	0.255	0.301	0.308	0.292	0.273
	(0.051)	(0.054)	(0.054)	(0.054)	(0.057)
10 hot days	−0.041	−0.036	−0.034	−0.034	−0.034
× decades	(0.029)	(0.032)	(0.033)	(0.034)	(0.035)
10 cold days	−0.036	−0.037	−0.034	−0.029	−0.024
× decades	(0.027)	(0.026)	(0.026)	(0.026)	(0.028)
Adjusted R^2	0.713	0.714	0.714	0.714	0.713

Notes: $N = 1,117,358$. Unit of analysis: counties × years × months. The two-tailed model (Eq.(A3)) is estimated using hot days (≥75°F) and cold days (<50°F), interacted with a continuous measure of decades since 1990. Rainy days are controlled for, along with county fixed effects and year-month fixed effects. Regressions are weighted by the log of labor force; standard errors clustered by commuting zone.

III Appendix: Quantitative Assessment

Cumulative lagged effects. To compute the total impacts of extreme temperature, we sum up lagged effects from previous months estimated earlier in Table A-4. For the purpose of quantifying the aggregate climate impacts, we rely on a parsimonious two-tailed model because bin models with lagged treatments are estimated much less precisely due to their large number of variables.[25] We construct the counterfactual unemployment rates over 1990–2019 (study period) where all the days fell into normal (non-hot, non-cold) days, which shall be compared with the observed unemployment rates to assess the role of extreme temperature. Figure A-10(a) presents the simulation results using lag distributions of up to M months ($M \in \{0,\cdots,5\}$). Incorporating lagged effects over $M = 0$ to $M = 4$ months systematically increases the implied reduction in the unemployment rate absent extreme temperatures.

To assess how climate change induced the shrinkage of unemployment volatility, we construct the counterfactual unemployment rates over 2000–2019 where the distribution of hot days and cold days remained in the averaged over the pre-warming 1950–1979. Then, we compute its within-year variance, which shall be compared with the observed data counterpart to assess the role of climate change. Figure A-10(b) reports the results using lag distributions of up to M months ($M \in \{0,\cdots,5\}$). Adding lags does not materially increase the implied contribution of climate change.

Figure A-10: Simulated Impacts across Treatment Lags

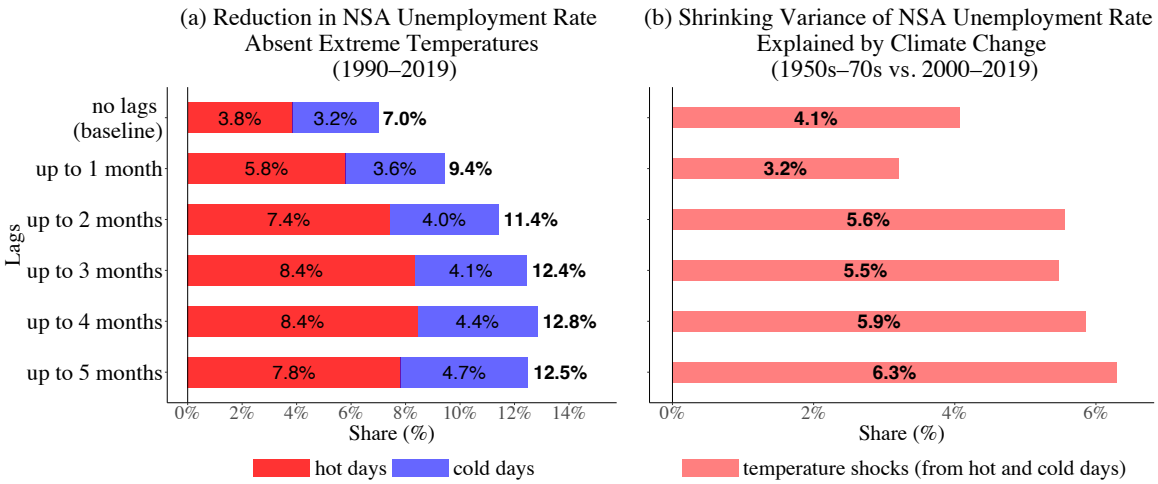

Notes: Simulations are based on a two-tailed model (Eq.(A3)) that includes hot days (≥75°F), cold days (<50°F) under a different lag distribution. An analogously lagged series of rainy days is controlled for, along with county fixed effects and year-month fixed effects. Regressions are weighted by the log of the labor force. See above for the simulation procedure.

[25] We find that climate impacts are mechanically underrated when using more extreme and rarer temperature thresholds (e.g., 85°F or 40°F) than the baseline cutoffs (i.e., 75°F or 50°F). These results are available upon request.

Robustness. Figure A-11 tests the robustness of the back-of-the-envelope calculations under key modeling protocols. As a preferred benchmark for quantitative assessment, Model (1) uses a two-tailed specification with up to two months of lags, as reported in Column 3 of Table A-4. Model (2) additionally controls for state-year fixed effects. Models (3) and (4) are bin-model counterparts to Models (1) and (2), respectively. Using bin models yields comparable implied effects of extreme temperatures in Panel (a), but noticeably larger effects in Panel (b). However, once lagged temperature bins are included, estimates become substantially less precise, and we thus refrain from using these specifications for our baseline simulation.

Figure A-11: Simulated Impacts across Key Modeling Protocols Under a Quarterly Treatment Window

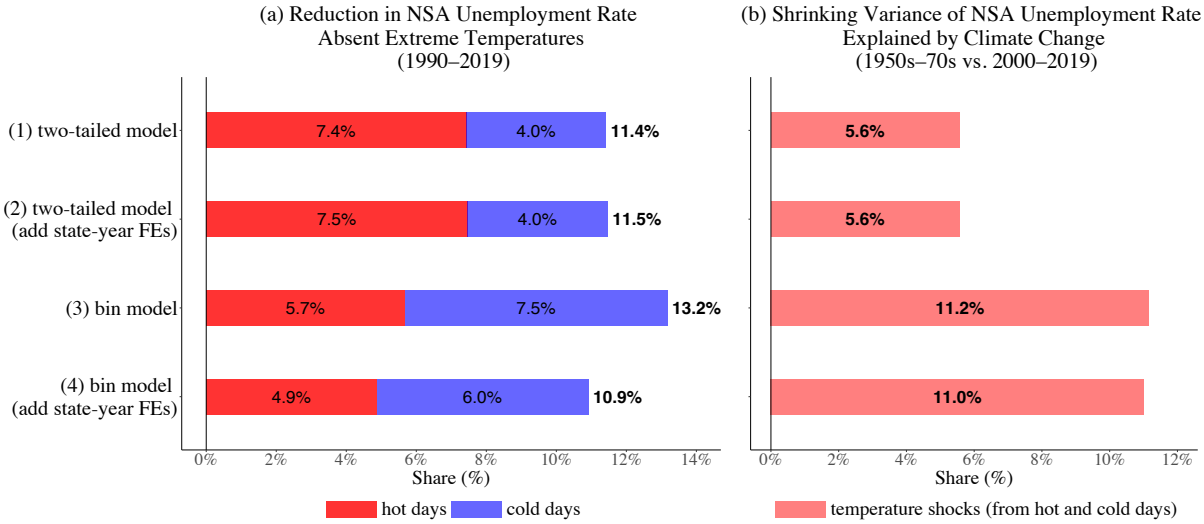

Notes: Simulations are based on two models: a two-tailed specification (Eq.(A3)) that includes hot days ($\geq$ 75°F) and cold days ($<$ 50°F), and a bin specification (Eq.(1)) that includes hot-day bins (13th–16th) and cold-day bins (1st–7th), with lags of up to two months for temperature variables. An analogously lagged series of rainy days is controlled for, along with county fixed effects and year-month fixed effects. Regressions are weighted by the log of the labor force. Panel (a): Monthly exposure to hot days and cold days over 1990–2019 is aggregated using a weighted sum with the vector of lagged coefficients. Panel (b): A difference of average monthly exposure to hot days and cold days between 1950–1979 and 2000–2019 is aggregated using a weighted sum with the vector of lagged coefficients. See Section III for the simulation procedure.

Within-year climate impacts. Using a two-tailed model with up to two months of lagged weather variables (Column 3 of Table A-4), Figure A-12 revisits the average within-year monthly climate impacts. Figure A-12(a) shows the climate impacts on NSA unemployment rates over 1990–2019. We find that the effects of additional hot and cold days are concentrated in the summer (Q3) and winter (Q1) quarters, respectively. The contribution of extreme temperatures to non-recessionary NSA unemployment exhibits substantial seasonal dispersion, ranging from 7.6% in May to 17.8% in September. Figure A-12(b) shows the impacts from climate change

from 1950s–1970s to 2000–2019. We find that fewer cold days reduce the unemployment rate in winter (Q1), while more hot days increase it in summer (Q3) and fall (Q4).

Figure A-12: Simulated Impacts on the NSA Unemployment Rate across Months

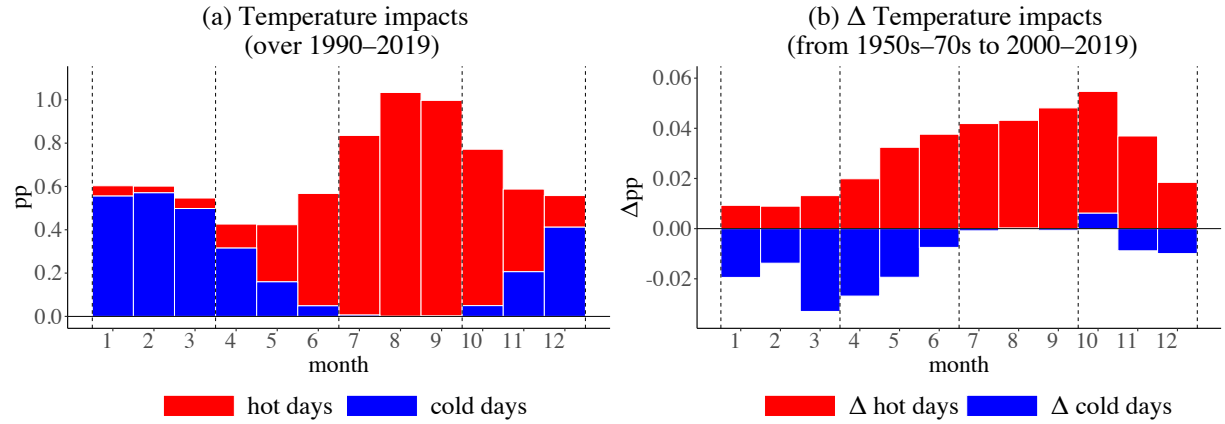

Notes: Simulations are based on a two-tailed model (Eq.(A3)) that includes hot days ($\geq$75°F) and cold days ($<$ 50°F), with lags of up to two months. An analogously lagged series of rainy days is controlled for, along with county fixed effects and year-month fixed effects. Regressions are weighted by the log of the labor force. Panel (a): Monthly exposure to hot days and cold days over 1990–2019 is aggregated using a weighted sum with the vector of lagged coefficients. Panel (b): A difference of average monthly exposure to hot days and cold days between 1950–1979 and 2000–2019 is aggregated using a weighted sum with the vector of lagged coefficients. See Section III for the simulation procedure.

IV Appendix: Mechanism

Definitions of flow proxies. For Table 1(a), we use the following proxies from the QWI based on the QWI codebook (QWI 101).

- **End-of-Quarter Employment Counts** (`EmpEnd`): Estimated number of jobs on the last day of the quarter.
- **Job creation** (`FrmJbGn`): Estimated number of jobs gained at firms throughout the quarter.
- **Job Destruction** (`FrmJbLs`): Estimated number of jobs lost at firms throughout the quarter.
- **End-of-Quarter Hires** (`HirAEnd`): Estimated number of workers who started a new job in the specified quarter, which continued into next quarter.
- **Separations (Stable)** (`SepS`): Estimated number of workers who had a job for at least a full quarter and then the job ended. Jobs are counted as a stable separation in the last quarter of employment.

For Table 1(b), we use the following proxies from the JOLTS based on the technical notes in the BLS News Release.

- **Hires**: include all additions to the payroll during the entire reference month, including newly hired and rehired employees; full-time and part-time employees; permanent, short-term, and seasonal employees; employees who were recalled to a job at the location following a layoff (formal suspension from pay status) lasting more than 7 days; on-call or intermittent employees who returned to work after having been formally separated; workers who were hired and separated during the month, and transfers from other locations.
- **Separations**: include all separations from the payroll during the entire reference month.
  - **Quits**: include employees who left voluntarily, with the exception of retirements or transfers to other locations.
  - **Layoffs and discharges**: includes involuntary separations initiated by the employer, including layoffs with no intent to rehire; layoffs (formal suspensions from pay status) lasting or expected to last more than 7 days; discharges resulting from mergers, downsizing, or closings; firings or other discharges for cause; terminations of permanent or short-term employees; and terminations of seasonal employees (whether or not they are expected to return the next season).
  - **Other separations**: include retirements, transfers to other locations, separations due to employee disability, and deaths.
- **Job openings**: include all positions that are open on the last business day of the reference month. A job is open only if it meets all three of these conditions:
  - A specific position exists, and there is work available for that position. The position can be full-time or part-time, and it can be permanent, short-term, or seasonal.
  - The job could start within 30 days, whether or not the employer can find a suitable candidate during that time.
  - The employer is actively recruiting workers from outside the establishment to fill the position.

V Appendix: Consequences for Unemployment Insurance

Descriptive statics: UI recipiency across states and months. Figure A-13 summarizes the descriptive statistics of UI recipiency. Figure A-13a illustrates our key variable of analysis: the state-level insured unemployment rate (i.e., the share of UI recipients in UI-covered employment) averaged over 1990–2019, shown in terms of its time trend (a1) and spatial dispersion (a2). The insured unemployment rate (solid line) comoves with the standard unemployment rate (dotted line), but with a smaller magnitude of about 1–4%. Moreover, the map (a2) shows that Northern states typically exhibit higher insured unemployment rates than Southern states, with notable exceptions such as South Dakota and California.

Figure A-13b documents monthly patterns in UI recipiency, comparing Northern and Southern states across three measures: (b1) the insured unemployment rate, (b2) average weekly benefits per UI recipient, and (b3) average monthly benefits paid per UI-covered employment. Two patterns emerge. First, the insured unemployment rate peaks primarily in winter (Q1) and secondarily in summer (Q3), mirroring the seasonal cycle of the standard unemployment rate (Recall Fact 1 in Section 2.3, Seasonal Regularity in Unemployment). Second, Northern states consistently exhibit higher UI recipiency than Southern states, likely reflecting differences in UI generosity.

Figure A-13: Descriptive Statistics of UI Recipiency

(a) Insured Unemployment Rate

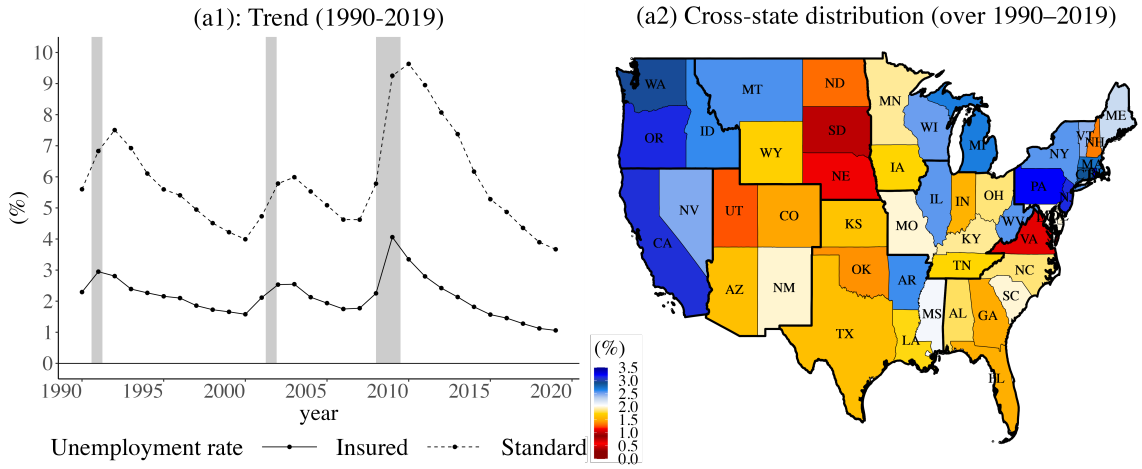

(b) UI Recipiency within a Year (over 1990–2019)

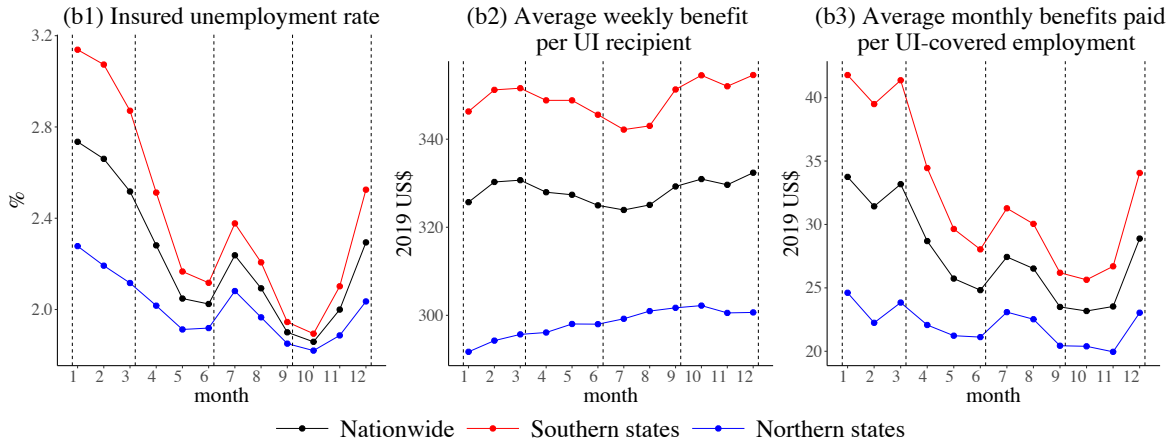

Notes: Panel (a1): Unemployment rates are headline statistics published by the BLS. The insured unemployment rate is defined as UI receipts divided by UI-covered employment. Panel (a2): Monthly NSA insured unemployment rates are averaged over 1990–2019, excluding NBER recession months. Bold black lines denote climatic zones defined by the NOAA. Panel (b) Southern states include the Southeast (VA, NC, SC, GA, AL, FL), South (TX, LA, MS, AR, OK, KS), Southwest (AZ, NM, UT, CO) and West (CA, NV). Northern states comprise the remaining contiguous U.S. states, including D.C. NBER recession months are excluded from the sample. Source: UI recipients are constructed by aggregating the Weekly Claims Data at the monthly level, while benefits paid, weekly benefits, and UI-covered employment are constructed from the Monthly Program and Financial Data, both produced by the Employment and Training Administration of the U.S. Department of Labor.

Climate impact on UI recipiency across states. Table A-8 examines the climate impact on UI recipiency across states over 1990–2019. Column 1 reports the key estimates of insured unemployment rate in Eq.(5): an additional 10 hot or cold days per month increase UI recipients by 0.11pp and 0.29pp per UI-covered employment, respectively. Columns 2–4 analyze alternative outcome variables using Eq.(5). Columns 2 and 3 show that claimed weeks and compensated weeks, respectively, are also responsive to extreme temperatures. Column 4 indicates that 10 hot or cold days per month raise UI expenditure by 0.95US$ and 4.39US$ per UI-covered employment, respectively. Columns 5–8 replace state fixed effects with state-year fixed effects; the estimates remain precisely estimated and generally larger in magnitude for hot days and smaller for cold days.

Table A-8: Extreme Temperature and Statewide UI Recipiency (Monthly, 1990–2019)

	Dependent variables			
	UI recipients (0–100 pp)	**Claimed weeks** (weeks)	**Compensated weeks** (weeks)	**benefits paid** (2019 US$)
	per UI-covered employment			
	(1)	(2)	(3)	(4)
	Descriptive statistics (mean (sd))			
	2.281	0.0866	0.0986	28.400
	(0.825)	(0.0346)	(0.0364)	(13.354)
10 hot days	0.105	0.00284	0.00272	0.946
	(0.034)	(0.00145)	(0.00125)	(0.374)
10 cold days	0.292	0.0143	0.0125	4.389
	(0.027)	(0.0012)	(0.0011)	(0.401)
state FEs	Yes	Yes	Yes	Yes
year × month FEs	Yes	Yes	Yes	Yes
Adjusted R^2	0.809	0.804	0.792	0.813
	(5)	(6)	(7)	(8)
10 hot days	0.161	0.00485	0.00470	1.615
	(0.032)	(0.00139)	(0.00119)	(0.361)
10 cold days	0.211	0.0114	0.00967	3.465
	(0.020)	(0.0009)	(0.00078)	(0.294)
state × year FEs	Yes	Yes	Yes	Yes
year× month FEs	Yes	Yes	Yes	Yes
Adjusted R^2	0.936	0.924	0.912	0.930

Notes: N = 17,640. Unit of analysis: states × years × months. Column 1 estimates the two-tailed model (Eq.(5)) using hot days (≥75°F) and cold days (<50°F). Columns 2–4 replace the outcome variable accordingly. Rainy days are controlled for. The regressions are weighted by the log of UI-covered employment; standard errors clustered by state. Source: UI recipients are constructed by aggregating the Weekly Claims Data at the monthly level, while claimed weeks, compensated weeks, benefits paid, and UI-covered employment are constructed from the Monthly Program and Financial Data, both produced by the Employment and Training Administration of the U.S. Department of Labor.

Simulated climate impacts on UI recipiency. Analogous to the unemployment impacts in Figure 4, Figure A-14 illustrates simulated impacts on insured unemployment. We use a two-tailed model (Eq.(5)) that includes hot days (≥75°F) and cold days (<50°F) with lags up to two months. By constructing a counterfactual in which all days are normal over 1990–2019, we quantify the contribution of extreme temperature. Figure A-14a reports impacts over 1990–2019 by temperature type and by Northern and Southern states. By constructing a counterfactual in which temperature shocks remain at their 1950s–70s averages, we then assess how much climate change has shifted insured unemployment in subsequent decades. Figure A-14b shows impacts for the 1980s, 1990s, 2000s, and 2010s relative to the 1950s–70s climate.

Figure A-14: Simulated Impacts on Insured Unemployment

(a) Impacts of Extreme Temperatures on the Insured Unemployment Rate (over 1990–2019)

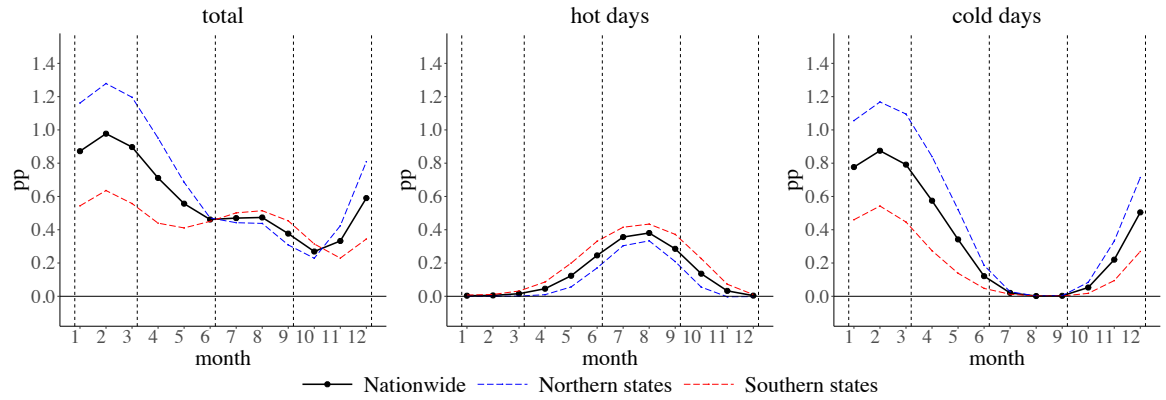

(b) Impacts of Climate Change since the 1950s–70s on the Insured Unemployment Rate

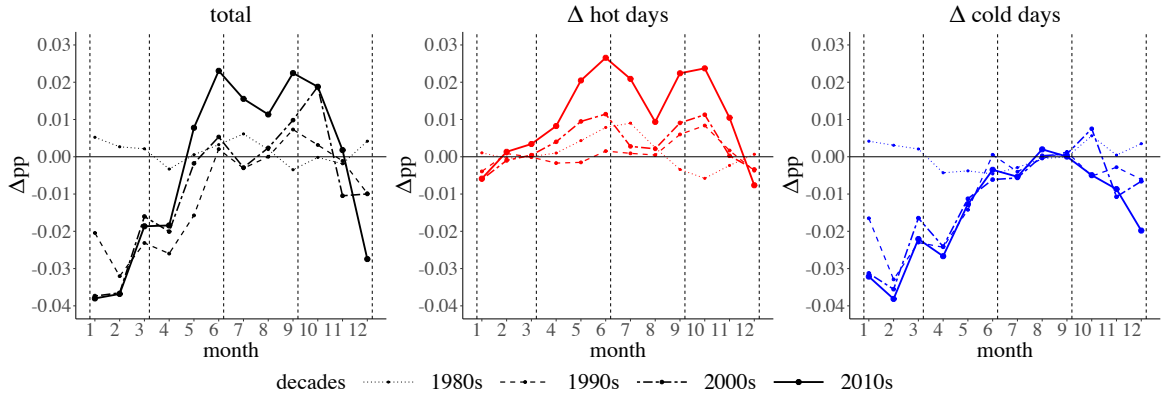

Notes: Simulations are based on a two-tailed model (Eq.(5)) that includes hot days (≥75°F) and cold days (<50°F) with lags of up to two months. An analogously lagged series of rainy days is controlled for, along with state fixed effects and year-month fixed effects. Regressions are weighted by the log of UI-covered employment. Panel (a): Monthly exposure to hot days and cold days over 1990–2019 is aggregated using a weighted sum with the vector of lagged coefficients. Southern states include the Southeast (VA, NC, SC, GA, AL, FL), South (TX, LA, MS, AR, OK, KS), Southwest (AZ, NM, UT, CO) and West (CA, NV). Northern states comprise the remaining contiguous U.S. states, including D.C. Panel (b): Decade-specific differences in average monthly exposure to hot and cold days, relative to the 1950s–1970s average, are aggregated using a weighted sum of lagged coefficients. Decades are defined as 1980–1989 (1980s), 1990–1999 (1990s), 2000–2009 (2000s), and 2010–2019 (2010s).

Within-year climate impacts. As in the earlier exercise on unemployment rate in Figure A-12, Figure A-15 revisits the simulated impacts on monthly insured unemployment rate. Using a two-tailed model (Eq.(5)) that includes hot days (≥75°F) and cold days (<50°F) with lags of up to two months, we apply the same simulation procedure as in Figure A-14. Figure A-15(a) shows the simulated climate impacts on insured unemployment rate over 1990–2019. Reflecting larger estimated coefficients for cold days, we find that the climate effects are concentrated in winter (Q1). Figure A-15(b) shows the simulated impacts of climate change between the 1950s–70s and 2000–2019. Fewer cold days in non-summer quarters (Q1–Q2, Q4) reduce insured unemployment, nearly offsetting those from more hot days outside winter (Q2–Q4).

Figure A-15: Simulated Impacts on NSA Insured Unemployment Rate across Months

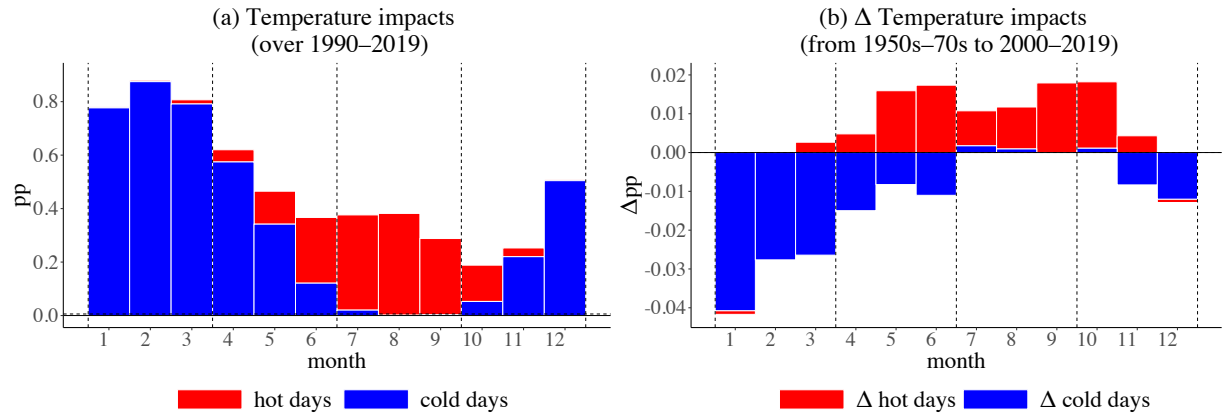

Notes: Simulations are based on a two-tailed model (Eq.(5)) that includes hot days (≥75°F) and cold days (<50°F), with lags of up to two months. An analogously lagged series of rainy days is controlled for, along with state fixed effects and year-month fixed effects. Regressions are weighted by the log of UI-covered employment. Panel (a): Monthly exposure to hot days and cold days over 1990–2019 is aggregated using a weighted sum with the vector of lagged coefficients. Panel (b): A difference of average monthly exposure to hot days and cold days between 1950–1979 and 2000–2019 is aggregated using a weighted sum with the vector of lagged coefficients.